Probing the acid sites of zeolites with pyridine: quantitative AGIR measurements of the molar absorption coefficients

Supplementary Information

Vladimir Zholobenko [a,b] *, Cátia Freitas [b], Martin Jendrlin [b], Philippe Bazin [a], Arnaud Travert [a], Frederic Thibault-Starzyk [a]

[a] Normandie Univ, ENSICAEN, UNICAEN, CNRS, Laboratoire Catalyse et Spectrochimie, France

[b] School of Chemical and Physical Sciences, Keele University, United Kingdom

* Corresponding author: v.l.zholobenko@keele.ac.uk

Experimental

List of Materials.

BEA-12 (Zeolyst CP814E, NH_4-form, Si/Al=12.5)

BEA-19 (Zeolyst CP814C, NH_4-form, Si/Al=19)

ZSM-5-40 (Zeolyst CBV8014, NH_4-form, Si/Al=40)

ZSM-5-27 (NIST reference material RM8852, NH_4-form, Si/Al=27)

MOR-7 (Crosfield, NH_4-form, Si/Al=7.0)

MOR-10 (Zeolyst CBV21A, NH_4-form, Si/Al=10)

FAU-C (Crosfield, NH_4-form, Si/Al=2.6)

FAU-Z (Zeolyst CBV300, NH_4-form, Si/Al=2.6)

ɔ-alumina (Puralox, Sasol)

fumed silica (Sigma-Aldrich, 99.8%)

US-Y zeolite (Crosfield, Si/Al=6)

The ex situ calcination temperature (if any) is indicated in the sample name. For instance, BEA-12-600ºC refers to a CP814E zeolite calcined ex situ at 600ºC prior to further analyses, the latter may have included an in situ activation at 450ºC.

Details of the analytical procedures and instrumentation along with the characterisation data for the samples studied in this work, including XRD patterns, SEM images, NMR and FTIR spectroscopic data are presented below.

Powder X-ray diffraction (XRD) patterns were recorded on a Bruker D8 Advance diffractometer equipped with a LynxEye detector using Cu KŬ radiation at 40 kV and 40 mA at ambient temperature over the 2-ɗ angle range of 5-60º ($\lambda_{K\check{U}1}$=0.15406 nm and $\lambda_{K\check{U}2}$=0.15444 nm; Soller slit of 2.5º; step size of 0.02º; time per step of 2976 sec; no monochromator was used). The crystalline phases were matched by comparing the collected XRD patterns with those available in the literature.

TM3000 (Hitachi) scanning electron microscope (SEM) with energy dispersive X-ray analysis (EDX) was utilised to obtain the elemental composition of the catalysts.

The apparent surface areas of the catalysts were measured using the BET model for the P/P_o relative nitrogen pressure <0.04; their micropore volume and the pore size distribution were computed using the nonlinear density functional theory (NLDFT) model applied to the adsorption branch of the nitrogen adsorption isotherms, according to the recent IUPAC recommendations (M. Thommes, K. Kaneko, A.V. Neimark, J.P. Olivier, F. Rodriguez-Reinoso, J. Rouquerol and K.S.W. Sing, *Physisorption of gases, with special reference to the evaluation of surface area and pore size distribution (IUPAC Technical Report)*, Pure Appl. Chem., 2015, 87(9-10) 1051ï 1069). The

experiments were carried out on a Quantachrom Autosorb instrument. The values obtained were scaled to the mass of the activated samples.

The thermogravimetric analyses have been carried out using a Rheometric Scientific STA 1500 instrument. The sample mass change and the heat flow were measured as a function of temperature (ramped from 20 to 800°C at 10°C/min).

Solid-state NMR experiments were performed using a 500 MHz Bruker Advance III spectrometer operating at a Larmor frequency of 130.3 MHz for ^{27}Al and 99.3 MHz for ^{29}Si. Hydrated powdered samples were packed into 4 mm rotors. For ^{27}Al MAS NMR, spectra were acquired using a relatively short pulse length of 1 µs (i.e., a selective pulse of 10°), a recycle delay of 1 s and a spinning rate of 14 kHz. For ^{29}Si MAS NMR, spectra were acquired using a 30° pulse, a recycle delay of 20 s and a spinning rate of 12 kHz. Chemical shifts were referenced to 1 mol L^{-1} $Al(NO_3)_3$ solution for ^{27}Al and to TMS for ^{29}Si.

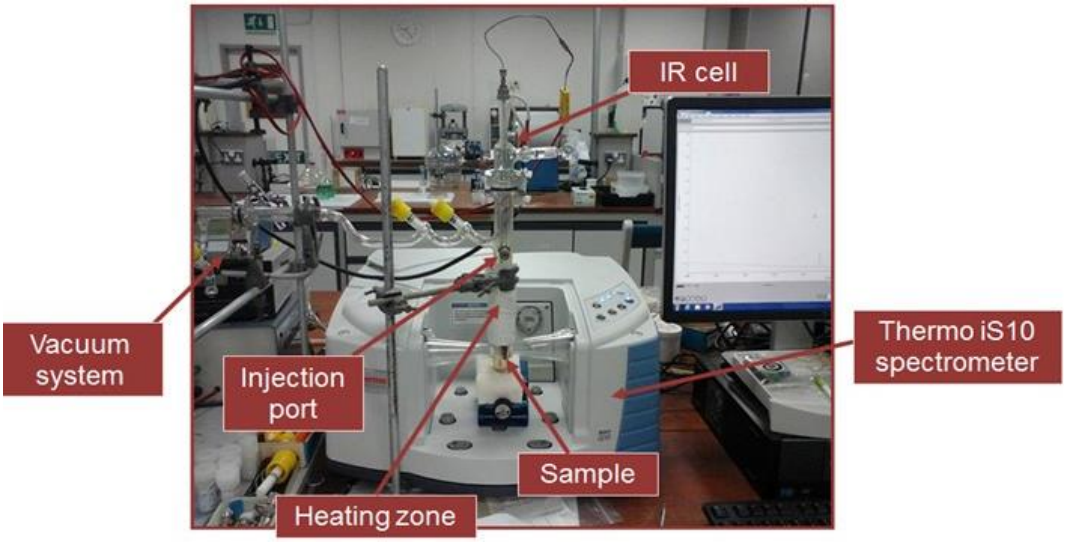

Figure S1. *In situ* FTIR spectroscopy set-up at Keele University.

Figure S2. AGIR set-up at LCS, Caen.

Results and Discussion

Preparation of the self-supported discs for FTIR measurements

The selected materials (e.g., silica, BEA and ZSM-5-40 zeolites) were pressed into self-supporting discs with the cross-section of S=1.3 cm^2, using a hydraulic bench press. The discs were made using a different mass (~2-40 mg), load (0, 1, 2, 5 and 8 tonnes) and time under load (1, 3, 5 and 120 sec). The SEM images were utilised to measure the thickness of the self-supporting discs. Figure S3 presents two SEM micrograph collected to obtain thickness data. Thickness of the disc decreases with increasing loads for all selected materials (fumed silica, BEA-12 and ZSM-5-40) and this effect is more noticeable for heavier discs (40 mg) (Figure S4). The changes are also observed when the discs are pressed at a different time under load, especially for the 40 mg discs. There are no significant changes in the thickness of the discs weighing ~10 mg after 5 seconds under pressure. These conclusions are similar for all materials selected for this study.

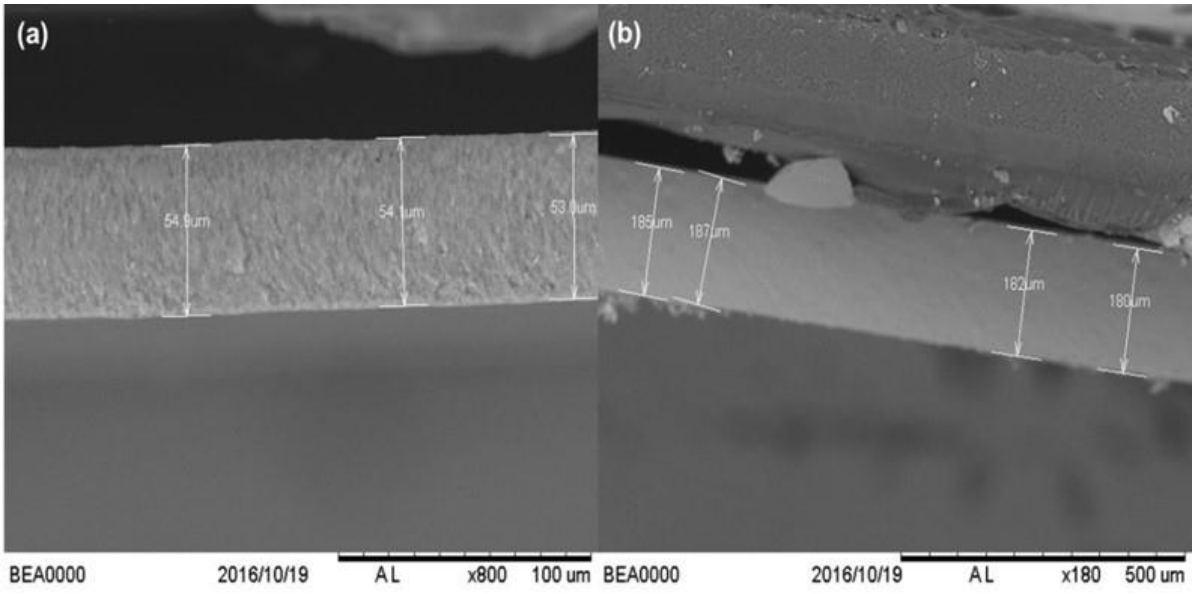

Figure S3. SEM micrograph of self-supported BEA-12 discs at different resolutions. **(a)** 10 mg BEA-12 sample prepared at an 8-tonne load for 1 sec and **(b)** 40 mg BEA-12 sample prepared at an 8-tonne load for 1 sec.

93

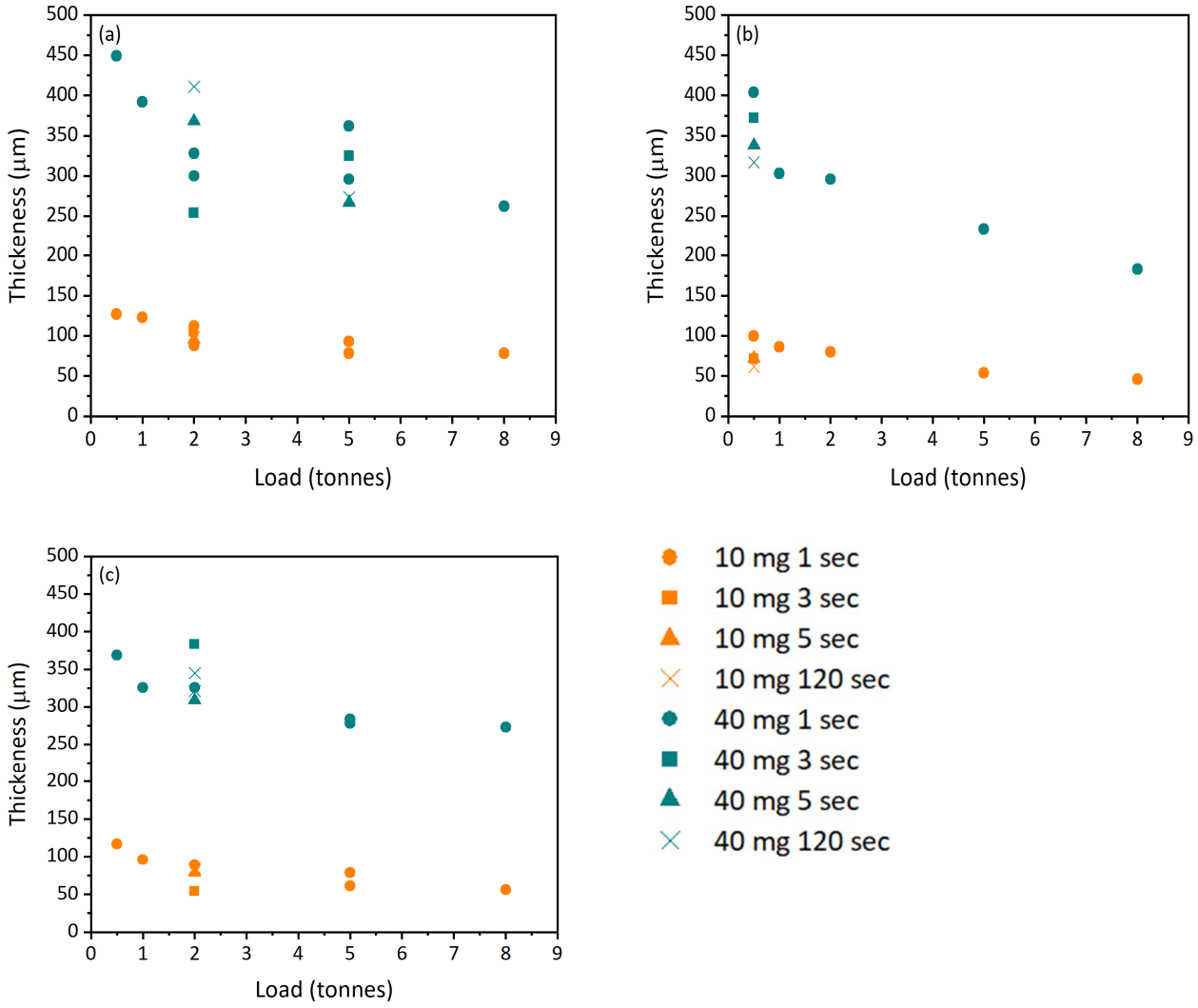

94

95 **Figure S4.** Thickness of the self-supporting discs prepared at different mass, load and time under
96 load. **(a)** fumed silica, **(b)** BEA-12, **(c)** ZSM-5-40 zeolites.

97

98

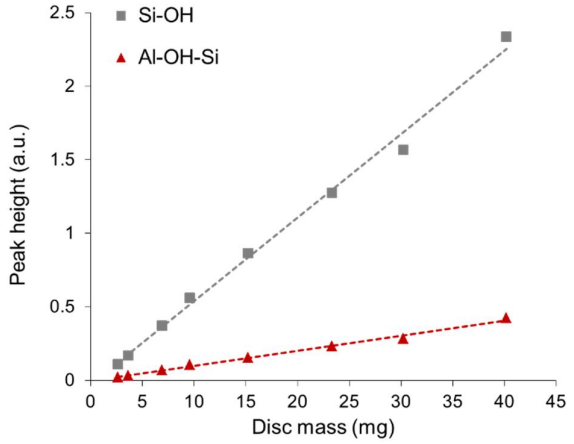

(a)

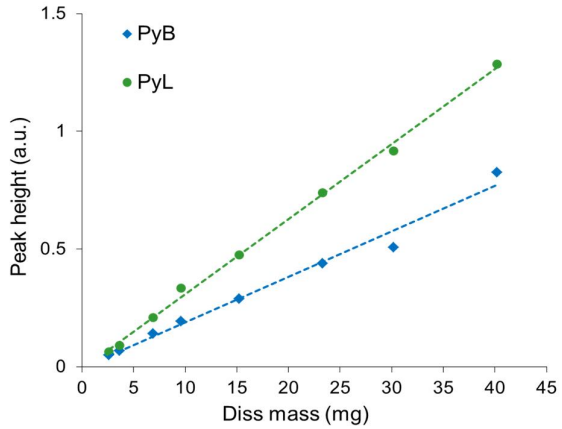

(b)

Figure S5. Linear relationship between the zeolite disc mass and the peak-height absorbance of the IR bands of (a) OH groups and (b) Py adsorbed on BAS and LAS in BEA-12 zeolite.

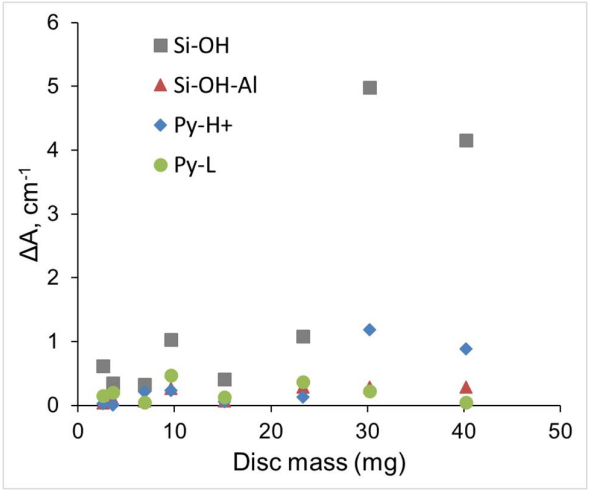

Figure S6. Deviation from the Beer-Lambert-Bouguer law for zeolite samples of different mass. (Based on the data presented in Figure 3; ΔA refers to peak area as in Figure 3.

99

Incomplete activation of the self-supporting sample discs prepared under the increasing load (0.5-8 tonnes) is evidenced by a decrease in the intensity of the Si-OH-Al peak at ~3610 cm^{-1} (subsequent Py adsorption shows a reduction in the intensity of the of Py-B peak at ~1545 cm^{-1}). This is due to the residual ammonia in the sample resulting from an incomplete activation during the pre-treatment step for discs prepared at excessively high loads (Figure S7). A similar, but not as pronounced, effect has been observed for discs with a lower mass (10 mg).

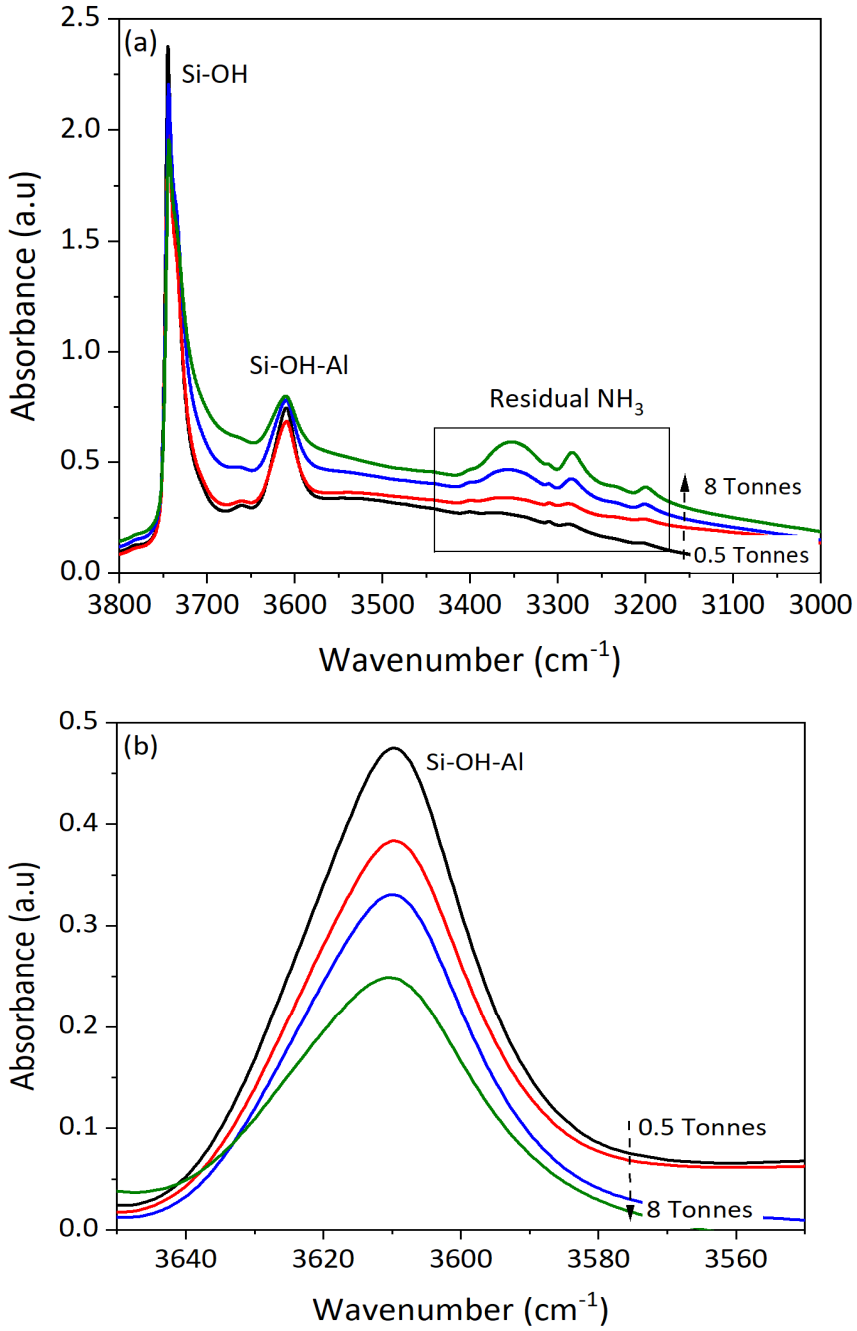

Figure S7. (a) FTIR spectra of the 40-mg BEA-12 discs prepared under different loads (0.5-8 tonnes) and activated at 450°C **(b)** FTIR spectra of the same samples showing the Si-OH-Al peak at ~3610 cm^{-1} (spectra collected at 90°C).

The CARROUCELL experiment. The results for five ZSM-5-40 and five BEA-12 zeolite samples are presented in Figures S8-S10 and Table S1.

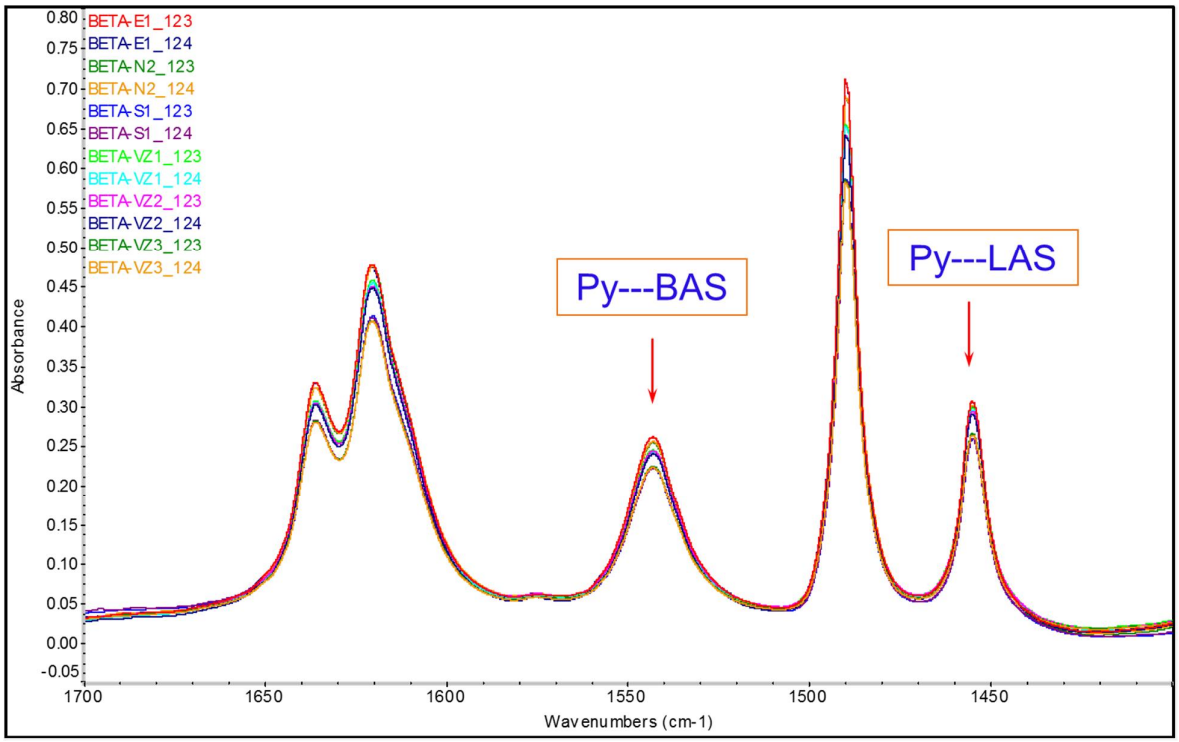

Figure S8. The CARROUCELL experiment: FTIR spectra of Py adsorbed on 5 samples of BEA-12. Two measurements were carried out for each sample (spectra collected at 150ºC).

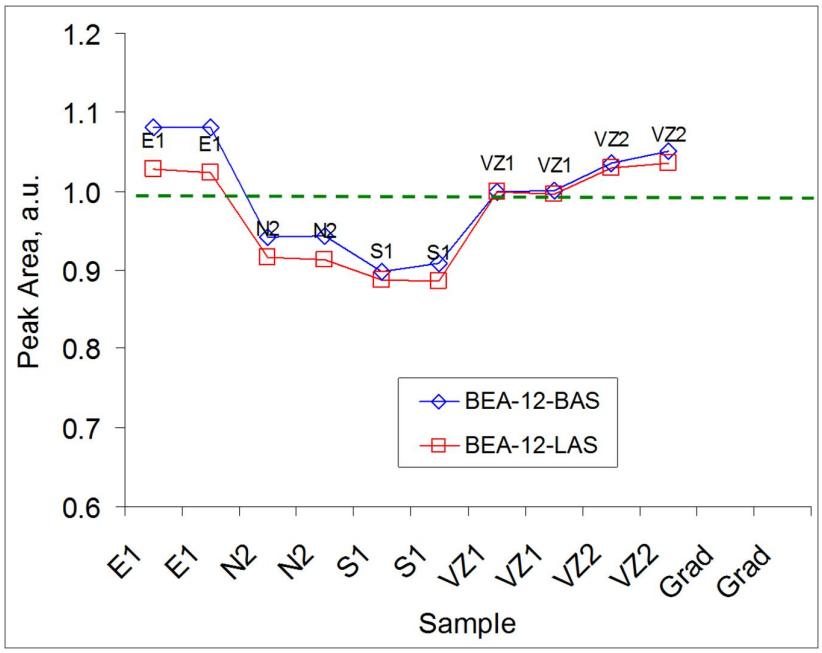

Figure S9. CARROUCELL experiment: normalised peak areas of Py-B and Py-L complexes on 5 samples of BEA-12. Two measurements were carried out for each sample. The pellets were made by different experimenters noted E, N, S and V.

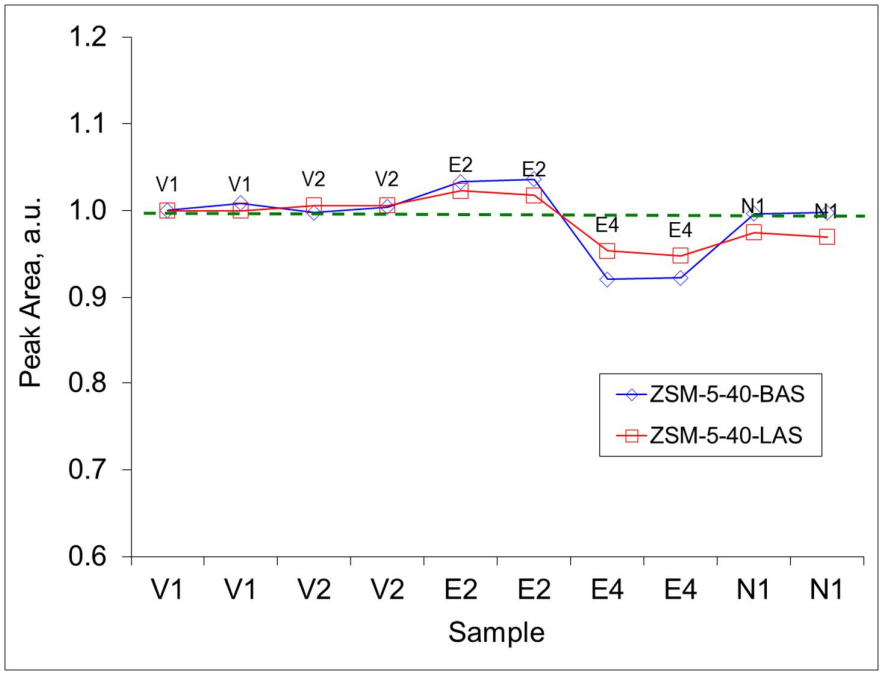

Figure S10. The CARROUCELL experiment: normalised peak areas of Py-B and Py-L complexes on 5 samples of ZSM-5-40. Two measurements were carried out for each sample. The pellets were made by different experimenters noted E, N, S and V.

Table S1. The mean and standard deviation values for the normalised peak areas of Py-B and Py-L complexes on ZSM-5-40 and BEA-12 zeolites from the CARROUCELL experiment (spectra collected at 150°C).

ZSM-5-40	**Py-B** ~1545 cm^{-1}	**Py-L** ~1455 cm^{-1}
Average	0.992	0.990
STDEVA	0.040	0.027
BEA-12	**Py-B**	**Py-L**
Average	0.994	0.972
STDEVA	0.068	0.063

Effect of the cell design.

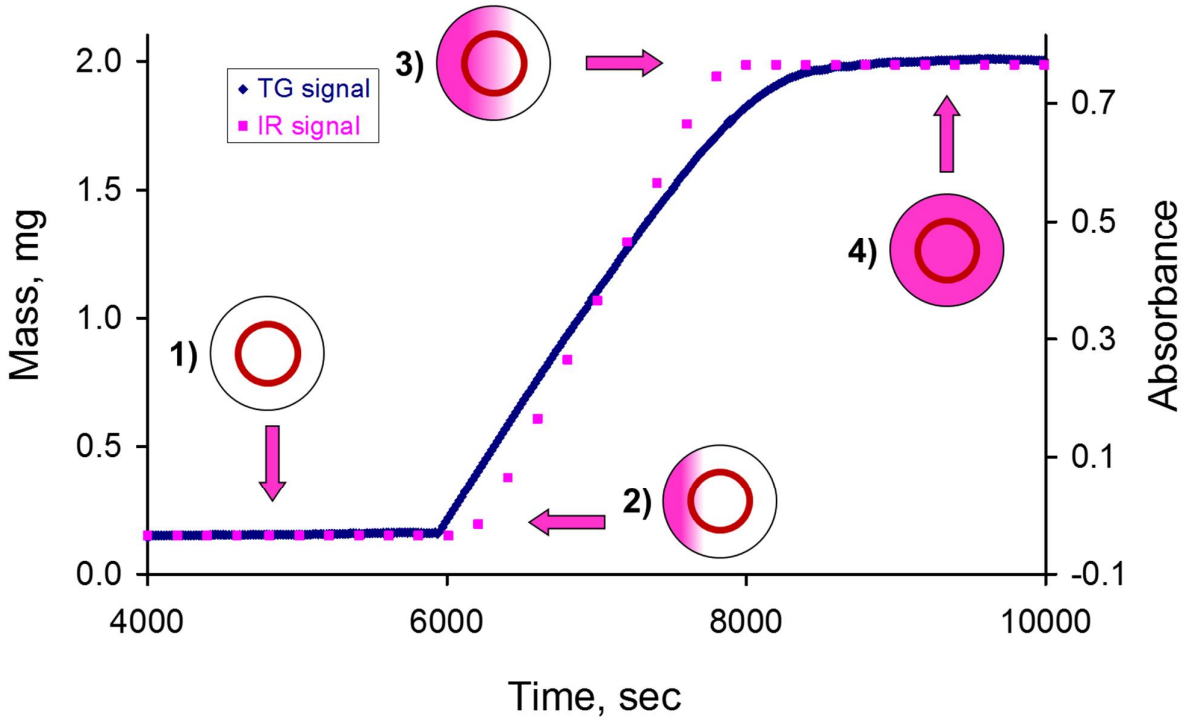

Figure S11. Schematic representation of Py adsorption on BEA-12: dynamics of the TG and IR signals (data collected at 200°C). 1) before Py adsorption, 2) initial stages of Py adsorption, 3) final stages of Py adsorption, 4) sample saturated with Py. The red circles show the border of the sample area probed by the infrared beam.

Effect of the resolution.

The effect of the spectral resolution on both Py-B and Py-L peaks is exemplified using Py adsorption at 150°C on BEA-19 (Figure S12). Integration of Py-B and Py-L peaks (Table S2) shows that in the spectra collected at 4 cm^{-1} there is a significant experimental error when the measurements are done by the peak height (~17% for Py-L). To reduce the experimental error, it is recommended to use measurements obtained by peak area instead of peak height as the peak area measurements are less affected by the resolution.

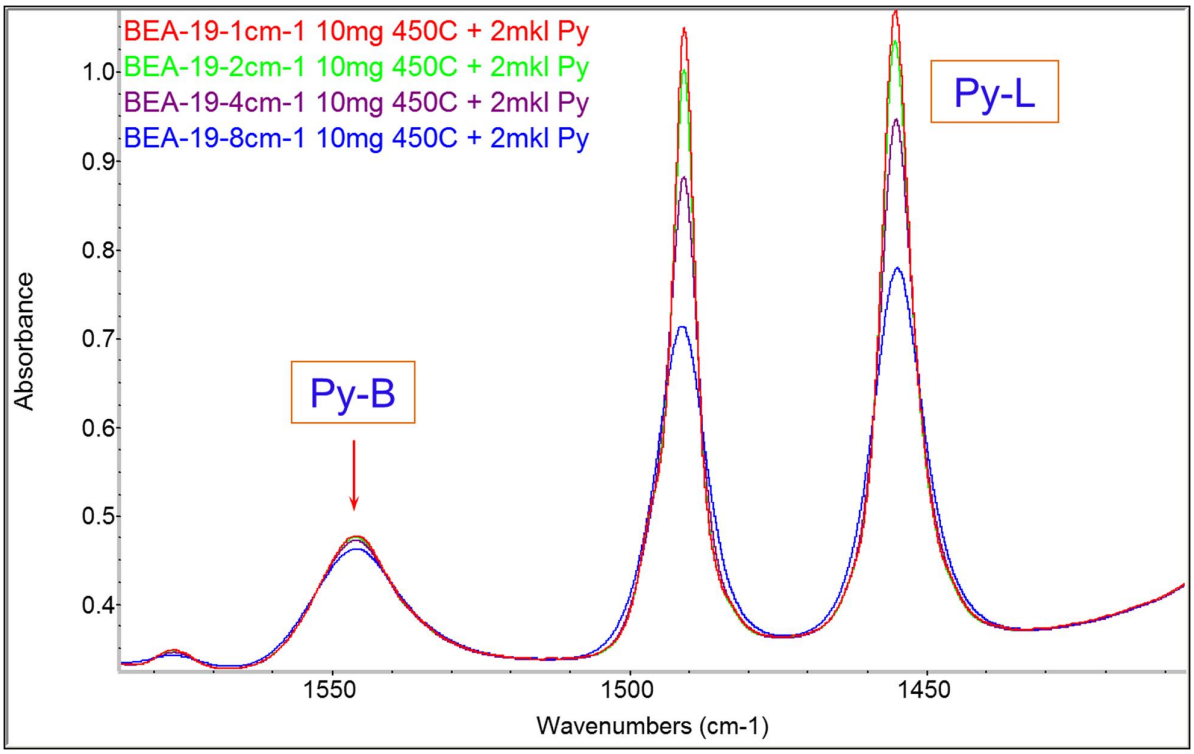

Figure S12. FTIR spectra of Py region following Py adsorption at 150°C on BEA-19. Spectra collected at different resolutions, from 1 to 8 cm^{-1} (spectra collected at 90°C).

Table S2. The peak areas and peak heights of Py-B and Py-L complexes in BEA-19 (at ~1545 and at ~1456 cm^{-1}, respectively) and associated experimental errors (figures **in bold**), taking the spectra collected at 1 cm^{-1} resolution as true value. FWHH is the full width at half-height of the peaks, see Figure S12 (spectra collected at 90°C).

Resolution cm^{-1}	**FWHH, cm^{-1}**		**Peak Area, cm^{-1}**		**Peak height, a.u.**	
	Py-B	**Py-L**	**Py-B**	**Py-L**	**Py-B**	**Py-L**
1	16.0	6.6	2.52	5.40	0.15	0.70
			-	-	-	-
2	16.2	6.8	2.51	5.30	0.14	0.67
			0.6%	**1.9%**	**0.7%**	**4.7%**
4	16.6	7.8	2.50	5.08	0.14	0.58
			0.6%	**5.9%**	**2.8%**	**17.1%**
8	18.0	10.7	2.43	4.63	0.13	0.41
			3.5%	**14.3%**	**10.3%**	**41.3%**

Effect of the temperature

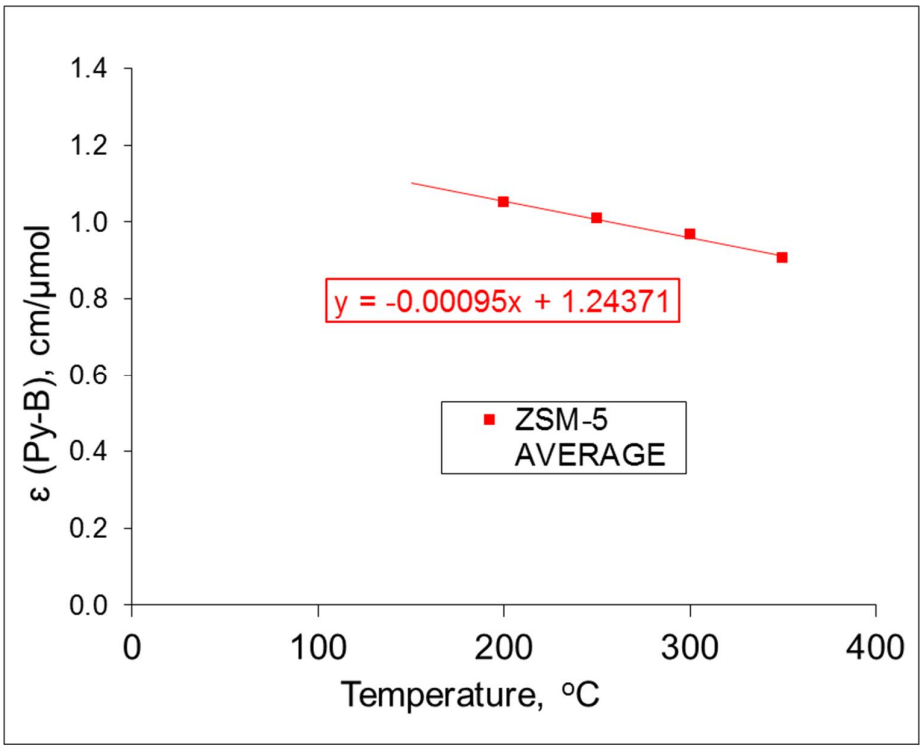

Figure S13a. The mean integrated molar absorption coefficient of Py-B complexes for ZSM-5 samples as a function of the temperature of the FTIR measurements.

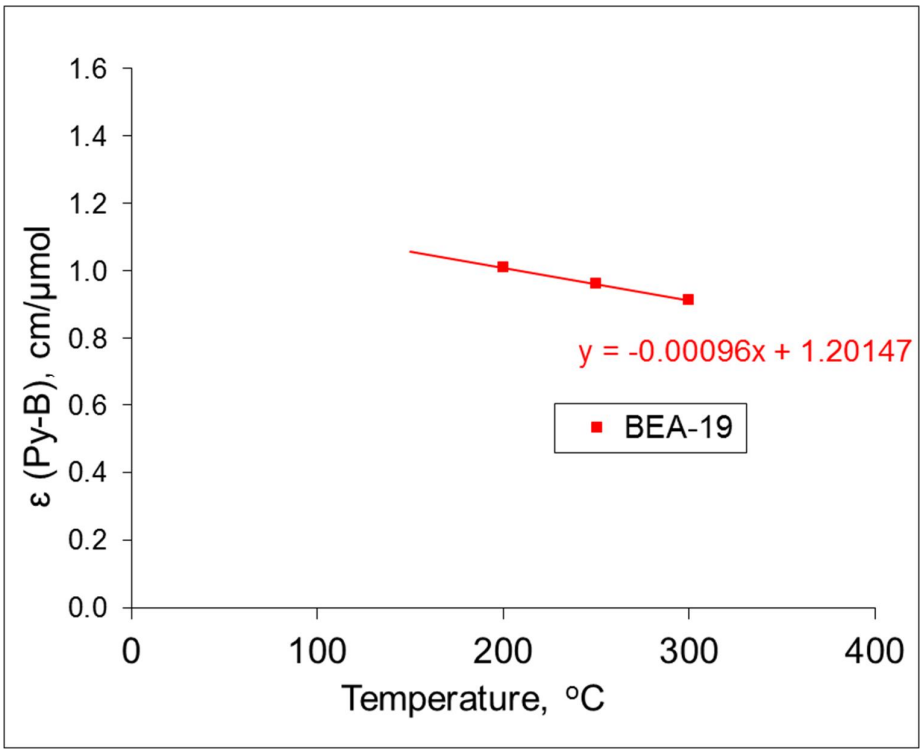

Figure S13b. The integrated molar absorption coefficients of Py-B complexes for BEA-19 as a function of the temperature of the FTIR measurements.

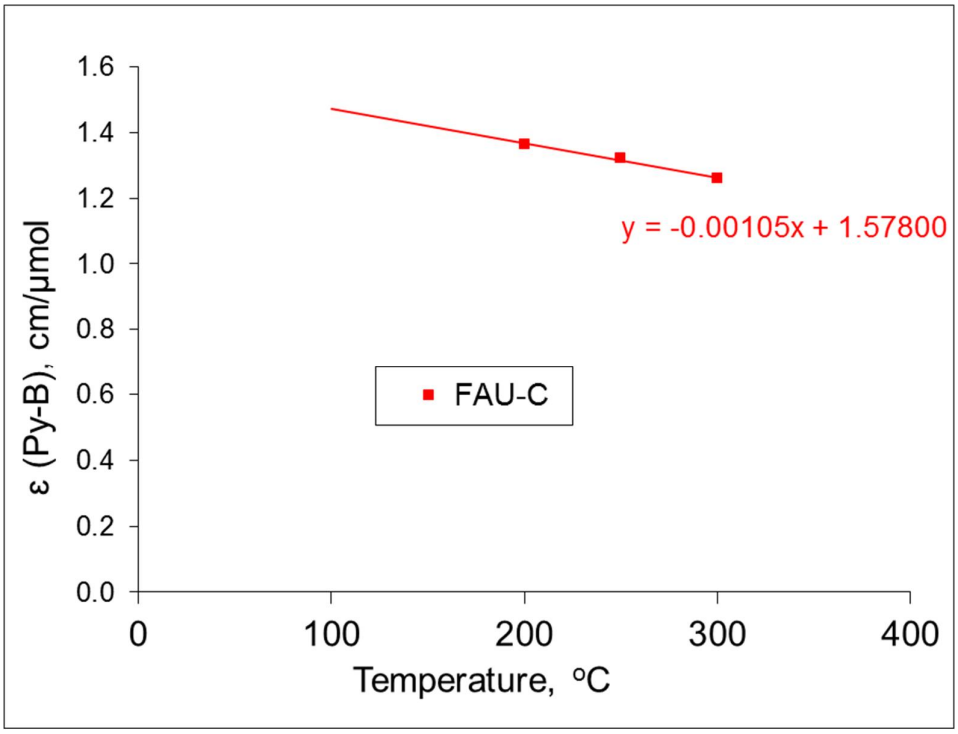

Figure S13c. The integrated molar absorption coefficient of Py-B complexes for FAU-C as a function of the temperature of the FTIR measurements.

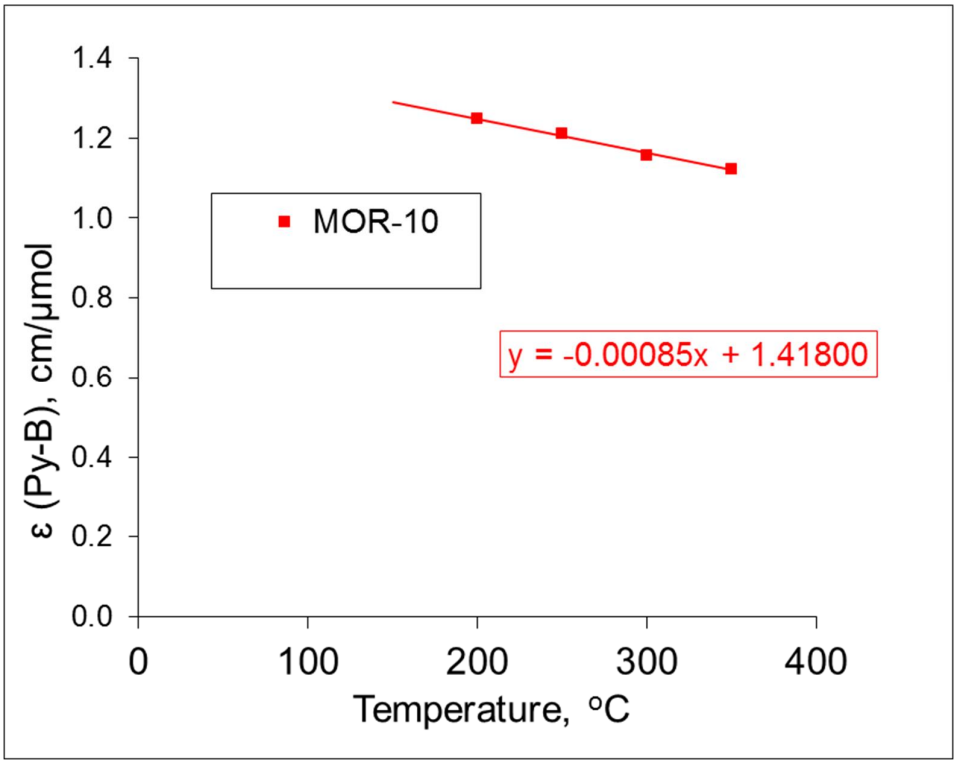

Figure S13d. The integrated molar absorption coefficient of Py-B complexes for MOR-10 as a function of the temperature of the FTIR measurements.

177

178 **Table S3**. Statistical data (ύ(Py-B) values, units = cm/ε mol), produced via repeated measurements
179 on different zeolite samples, for the integrated molar absorption coefficients of Py-B complexes
180 obtained by AGIR measurements at 200-350°C.

181

Sample		ZSM-5	ZSM-5	ZSM-5	ZSM-5	BEA-19	FAU-C
Temp, °C		200	250	300	350	200	200
ε (Py-B)	ZSM-5-40	1.044	0.993	0.931	0.905	0.940	1.36
cm/ε mol	ZSM-5-40	1.003	0.956	0.907	0.874	1.100	1.54
	ZSM-5-40	1.092	1.046	0.983	0.961	1.080	1.41
	ZSM-5-40	1.035	0.980	0.936	0.885	1.010	1.5
	ZSM-5-40	1.017	0.964	0.900		1.140	1.51
	ZSM-5-40	1.091	1.020	1.021		1.150	
	ZSM-5-40-600°C	1.064	1.085	1.067			
	ZSM-5-40-700 °C	1.084	1.044	1.000			
	ZSM-5-27	1.045	1.021	0.991			
	ZSM-5-27	1.029	0.977	0.949			
AVERAGE		**1.051**	**1.009**	**0.968**	**0.906**	**1.070**	**1.464**
STDEVA		**0.031**	**0.042**	**0.053**	**0.039**	**0.081**	**0.076**

182

183

Table S4. Statistical data for the peak positions of Py-B and Py-L complexes and of OH-groups (in cm^{-1}) on various zeolites obtained from AGIR measurements at 200-300°C.

Sample	ZSM-5-40	ZSM-5-40	ZSM-5-40	BEA-19	BEA-19	BEA-19	Sample	FAU-C	FAU-C	FAU-C	US-Y	US-Y	US-Y	MOR-10	MOR-10	MOR-10
Temp, oC	200	250	300	200	250	300	Temp, oC	200	250	300	200	250	300	200	250	300
Peak	1544.5	1543.4	1542.4	1544.0	1543.0	1542.3	Peak	1540.6	1540.0	1539.1				1542.8	1541.7	1540.7
Py-B	1544.1	1543.2	1542.3	1543.3	1542.8	1541.7	Py-B	1540.9	1540.2	1539.4				1542.9	1541.8	1540.8
cm-1	1544.5	1543.8	1542.8	1543.9	1543.0	1542.2	cm-1				1543.1	1542.3	1541.5			
	1544.2	1543.3	1542.5	1543.6	1542.6	1541.7					1542.3	1541.6	1541.0			
	1544.1	1543.3	1542.5													
	1544.2	1543.1	1542.1													
AVERAGE	1544.3	1543.4	1542.4	1543.7	1542.9	1542.0	AVERAGE	1540.8	1540.1	1539.3	1542.7	1542.0	1541.3	1542.9	1541.8	1540.8
STDEVA	0.19	0.24	0.23	0.32	0.19	0.32	STDEVA	0.21	0.14	0.21	0.57	0.49	0.35	0.07	0.07	0.07
Sample	ZSM-5-40	ZSM-5-40	ZSM-5-40	BEA-19	BEA-19	BEA-19	Sample	FAU-C	FAU-C	FAU-C	US-Y	US-Y	US-Y	MOR-10	MOR-10	MOR-10
Temp, oC	200	250	300	200	250	300	Temp, oC	200	250	300	200	250	300	200	250	300
Peak	1454.9	1454.6	1454.3	1454.7	1454.4	1453.9	Peak	1453.8	1453.5	1453.2				1454.0	1453.6	1453.2
Py-L	1454.6	1454.4	1454.2	1454.5	1454.1	1453.7	Py-L	1452.9	1452.4	1452.0				1453.9	1453.5	1453.0
cm-1	1455.1	1454.7	1454.3	1454.3	1453.9	1453.5	cm-1				1454.6	1454.3	1453.9			
	1455.7	1455.4	1454.8	1455.1	1454.7	1454.2					1454.1	1453.5	1453.1			
	1455.6	1454.9	1454.6													
	1455.9	1455.2	1454.6													
AVERAGE	1455.3	1454.9	1454.5	1454.7	1454.3	1453.8	AVERAGE	1453.4	1453.0	1452.6	1454.4	1453.9	1453.5	1454.0	1453.6	1453.1
STDEVA	0.51	0.38	0.23	0.34	0.35	0.30	STDEVA	0.64	0.78	0.85	0.35	0.57	0.57	0.07	0.07	0.14
Al(OH)Si LF								3546.3	3545.8	3545.1						
Al(OH)Si HF	3603.4	3601.3	3598.9	3605.0	3603.4	3601.3		3636.4	3634.6	3632.5				3603.1	3600.4	3597.6
SiOH	3738.1	3736.9	3735.6	3733.8	3732.9	3732.0		3742.1	3741.2	3740.2				3742.7	3741.8	3740.7

Experimental data for the samples containing both BAS and LAS.

By using the following equation, both ύ(Py-B) and ύ(Py-L) values have been determined from the gradient and the y-intercept of the trend lines.

$$\frac{A_B \times S}{n_{total}} = -\frac{\varepsilon_B}{\varepsilon_L} \times \frac{A_L \times S}{n_{total}} + \varepsilon_B$$

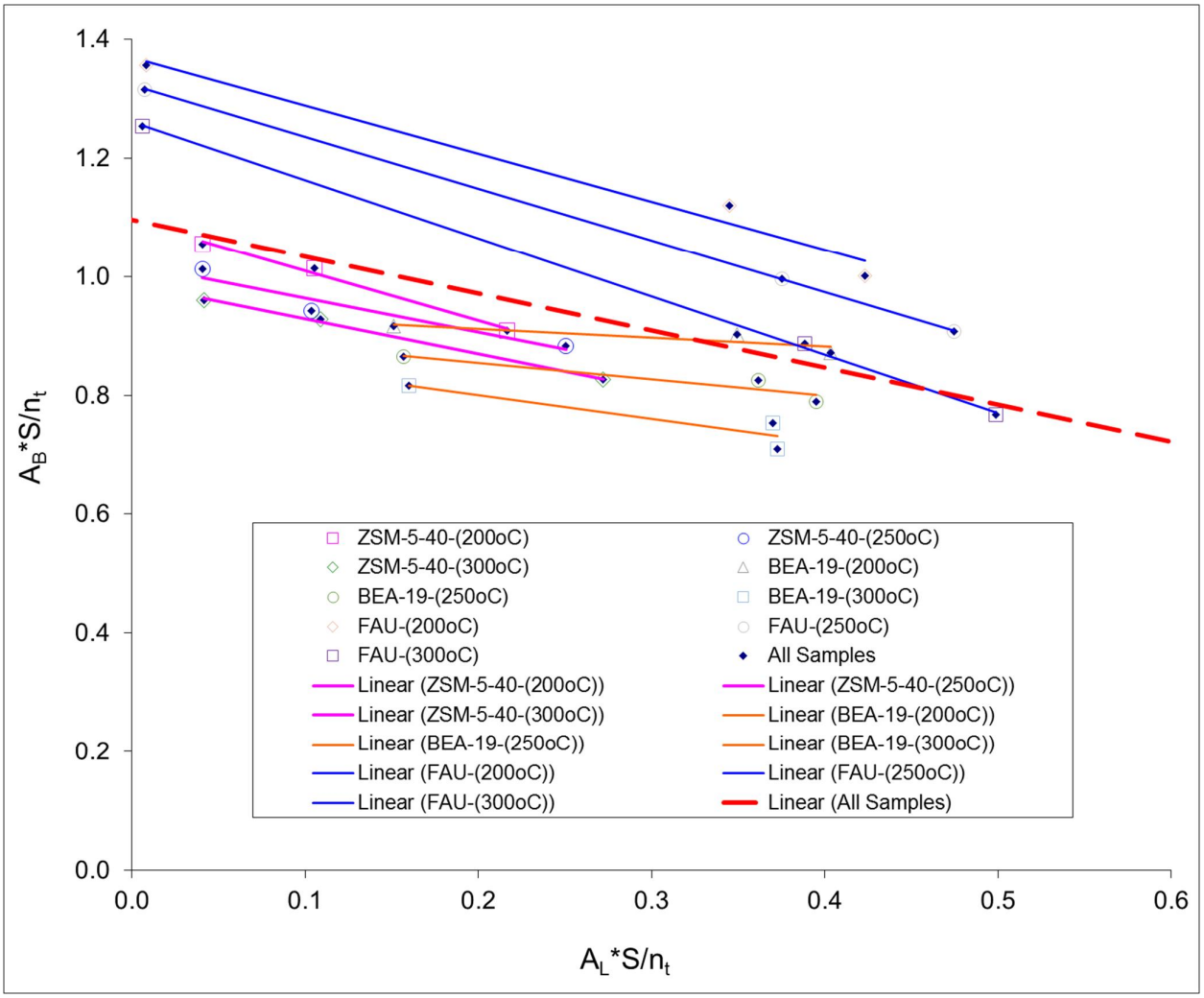

Figure S14. Characterisation of ZSM-5-40, BEA-19 and faujasite zeolite samples containing both Py-B and Py-L complexes. The temperature values in brackets indicate the temperature of the FTIR measurements.

Table S5. Statistical data, produced via repeated measurements, for the integrated molar absorption coefficients of Py-B and Py-L complexes on various zeolite samples with different ratio of BAS/LAS, obtained by AGIR measurements at 200°C (ύ(Py-B) and ύ(Py-L) values, units = cm/εmol).

Sample	ZSM-5-40		BEA-19		FAU	
	ε (Py-B)	**ε (Py-L)**	**ε (Py-B)**	**ε (Py-L)**	**ε (Py-B)**	**ε (Py-L)**
	1.06	1.66	0.94	6.38	1.41	1.72
	1.06	1.68	1.10	1.92	1.37	1.69
	1.07	1.51			1.41	1.73
	1.08	1.72				
Average	**1.07**	**1.64**	**1.02**	**4.15**	**1.39**	**1.71**
STDEVA	0.01	0.09	0.11	3.15	0.02	0.02

Appendix: Characterisation data for the samples studied in this work

XRD data

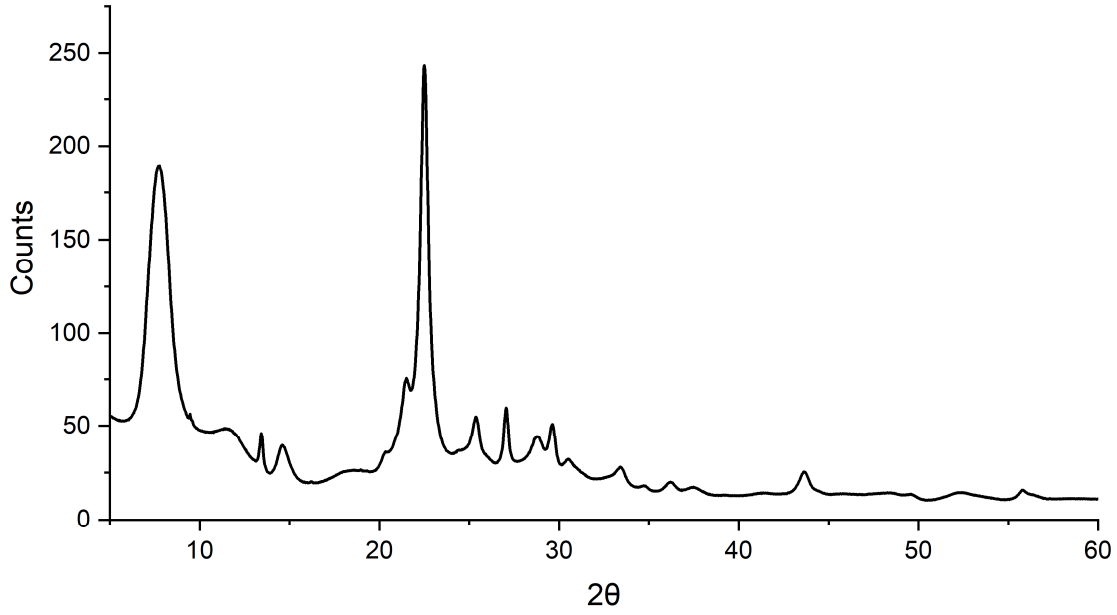

Figure S15a. XRD pattern of BEA-12.

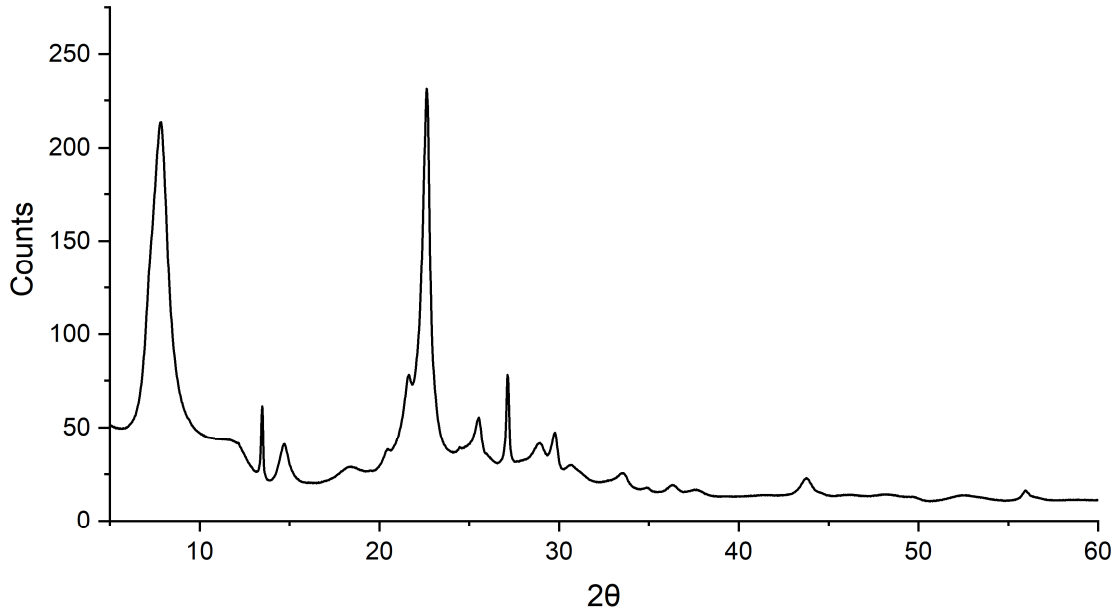

Figure S15b. XRD pattern of BEA-19.

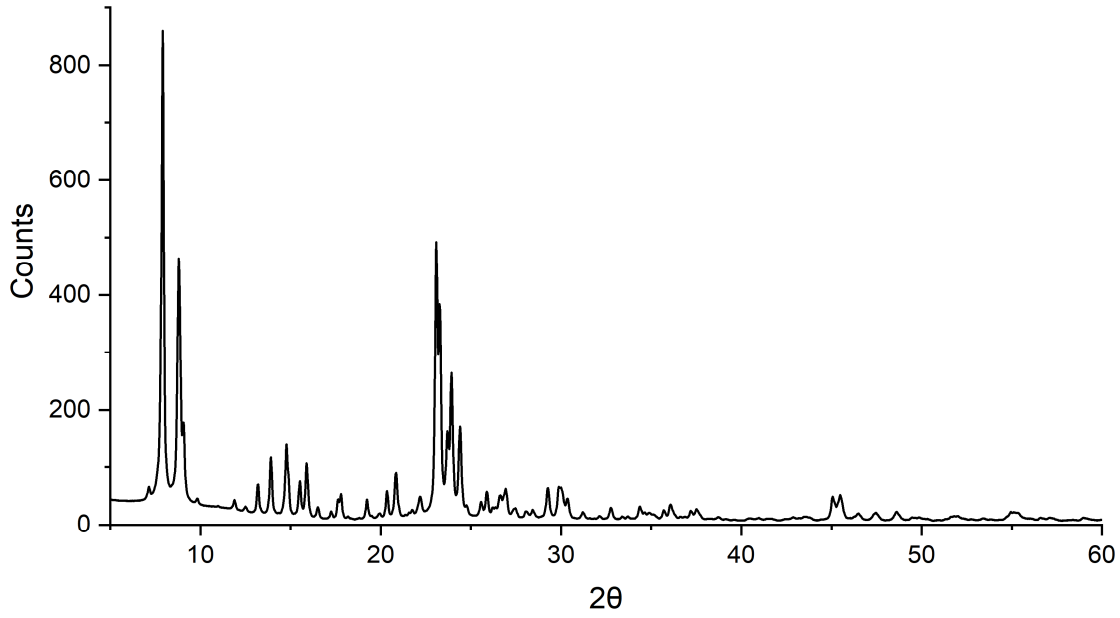

Figure S15c. XRD pattern of ZSM-5-40.

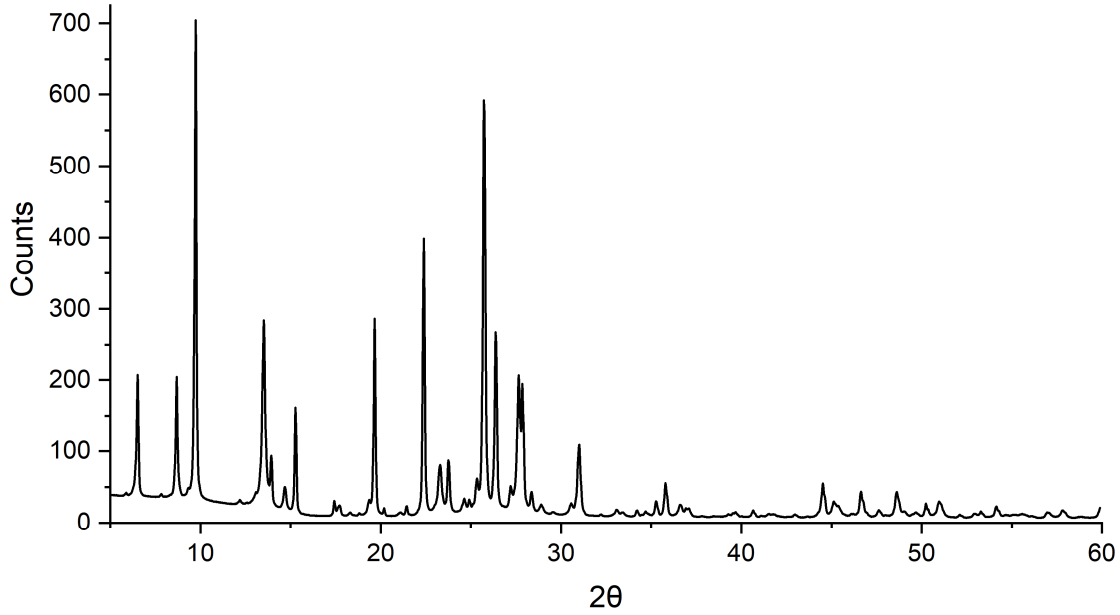

Figure S15d. XRD pattern of MOR-10.

215

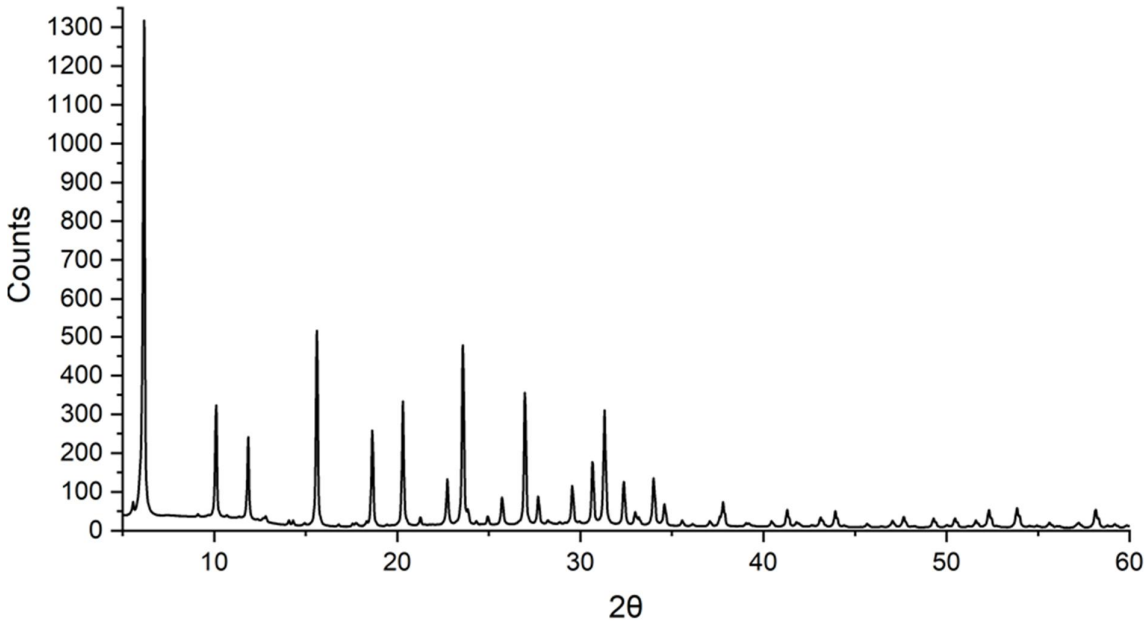

Figure S15e. XRD pattern of FAU-C.

216

217

218

219 **Nitrogen adsorption data**

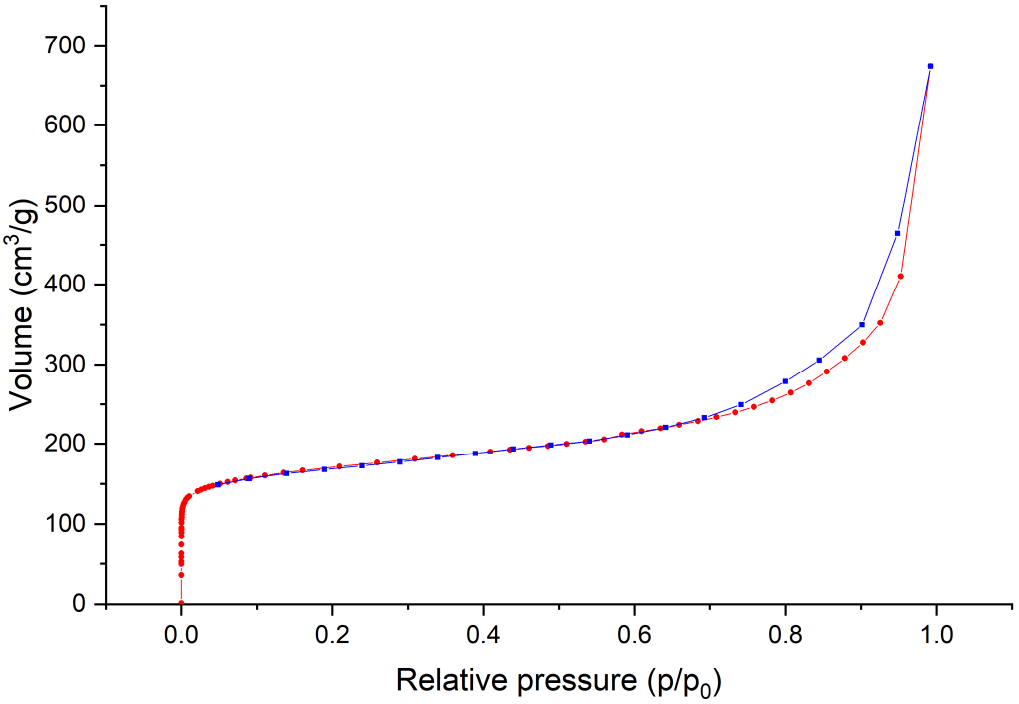

Figure S16a. Nitrogen adsorption-desorption isotherm for BEA-12.

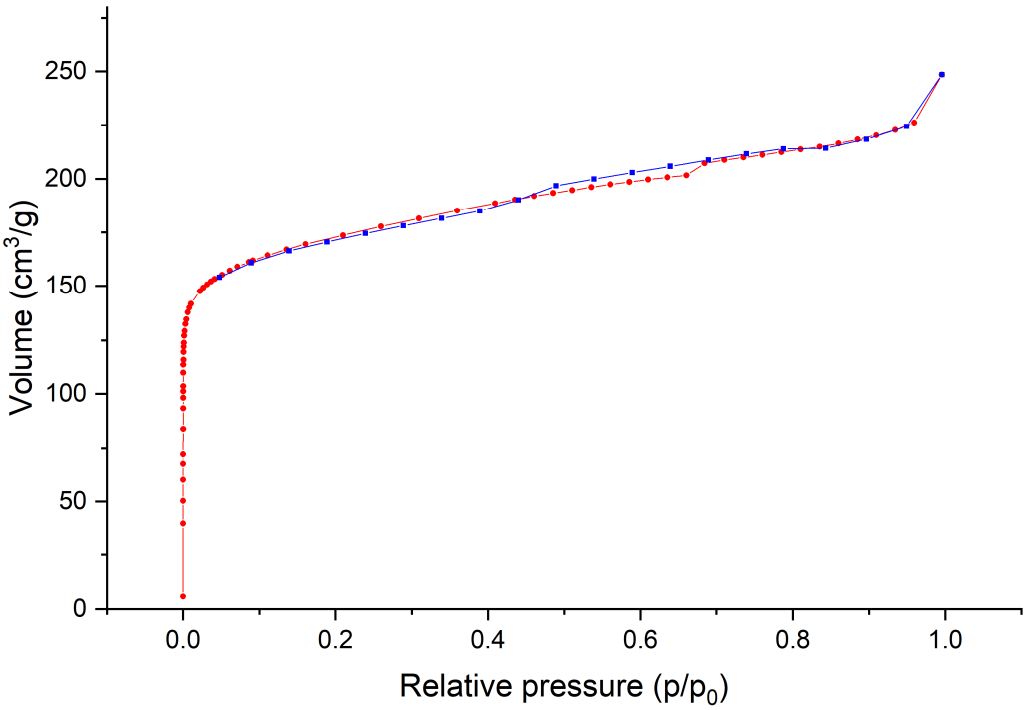

Figure S16b. Nitrogen adsorption-desorption isotherm for BEA-19.

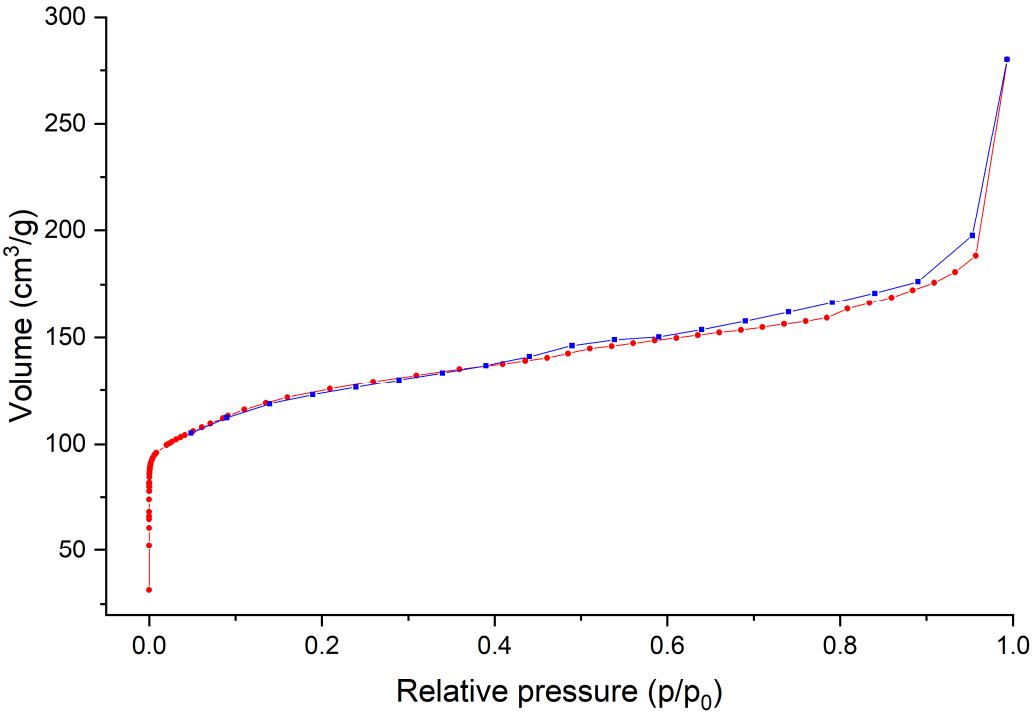

Figure S16c. Nitrogen adsorption-desorption isotherm for ZSM-5-40.

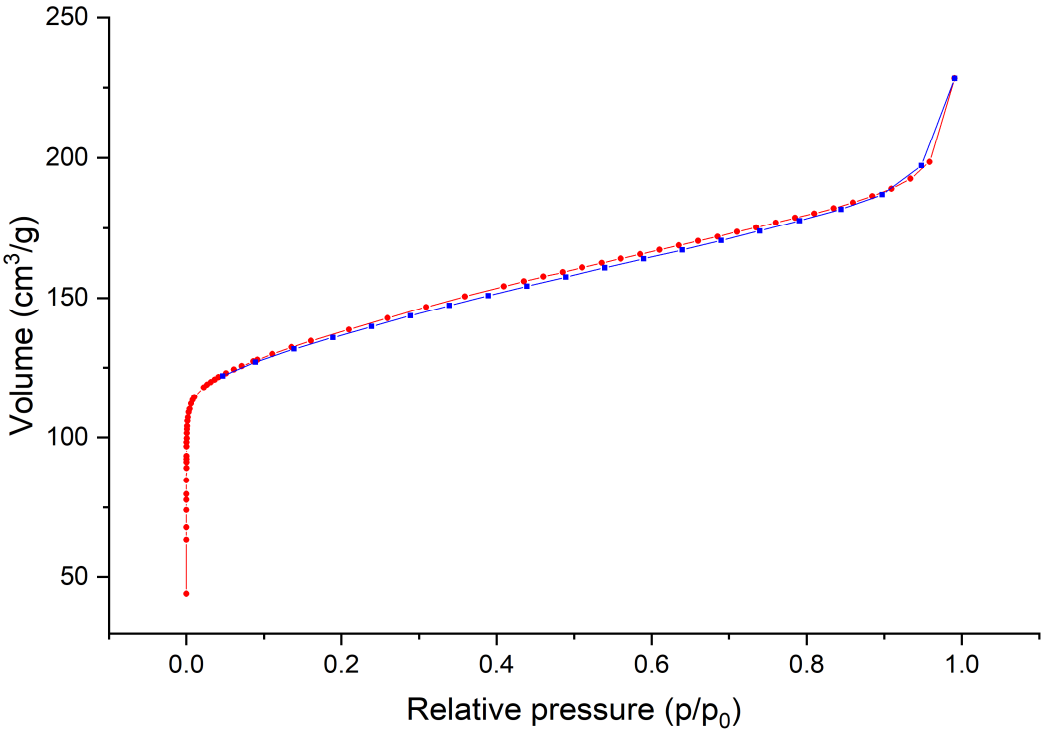

Figure S16d. Nitrogen adsorption-desorption isotherm for MOR-10.

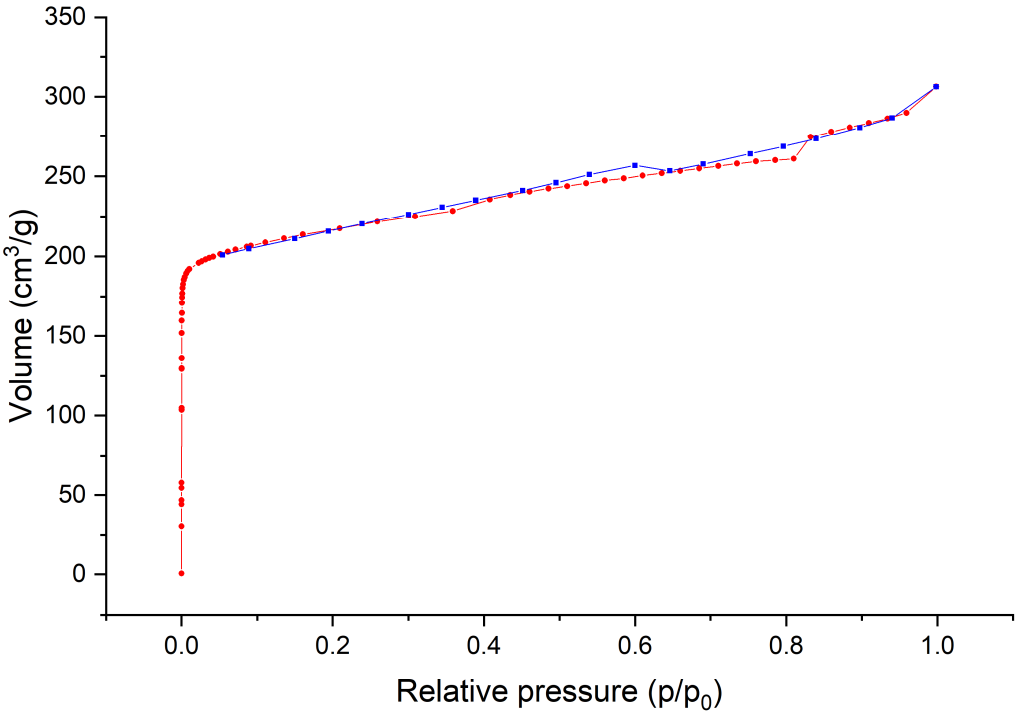

220 **Figure S16e.** Nitrogen adsorption-desorption isotherm for FAU-Z.

221

222

223 **TGA data**

224

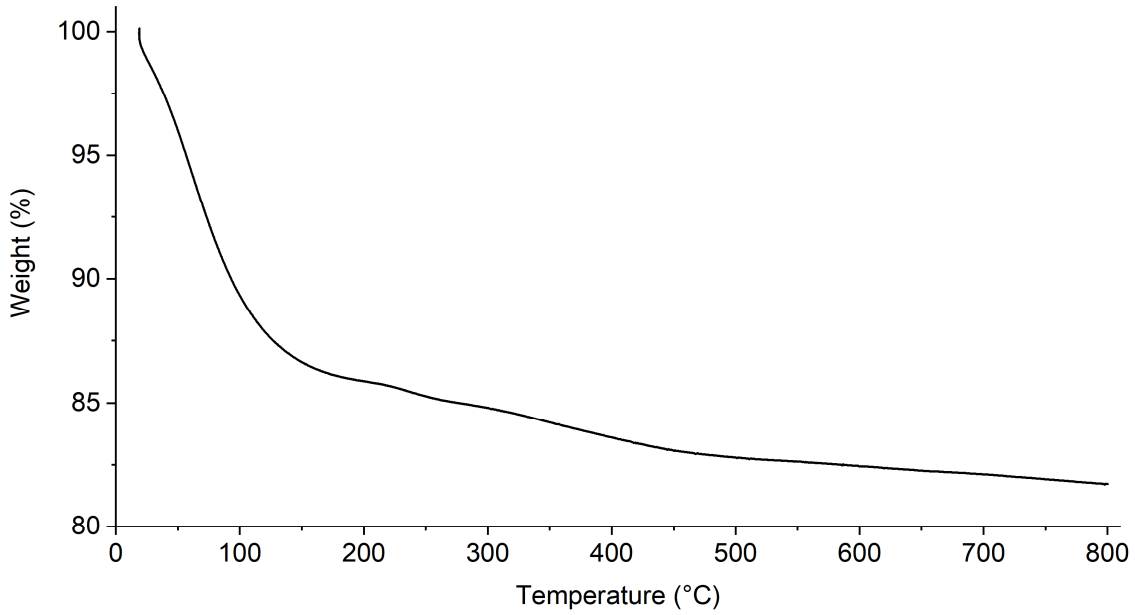

Figure S17a. Thermogravimetric analysis curve of BEA-12.

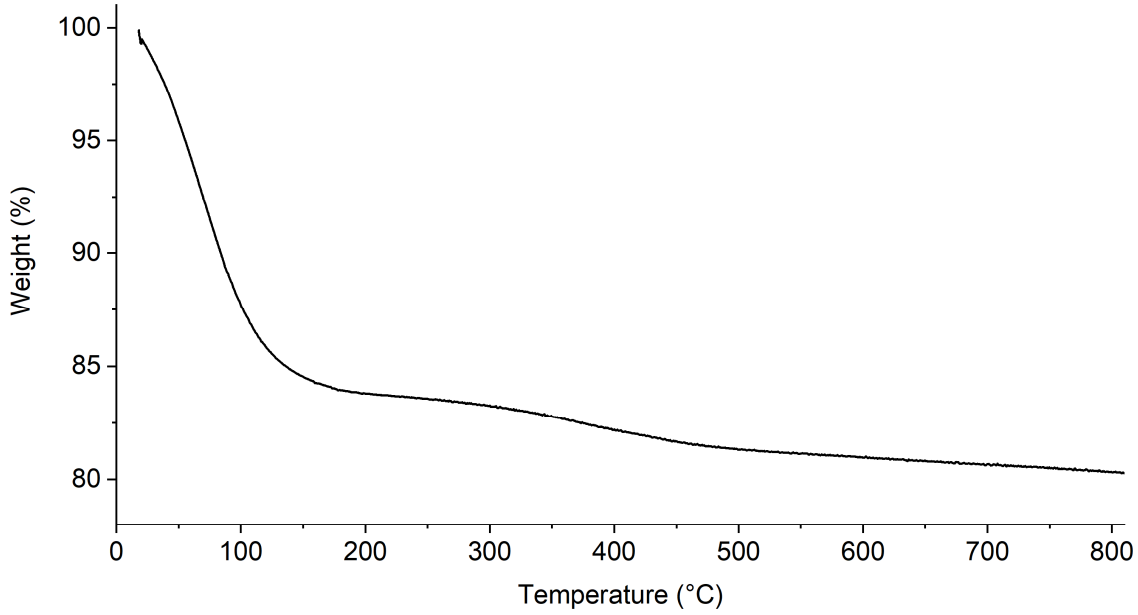

Figure S17b. Thermogravimetric analysis curve of BEA-19.

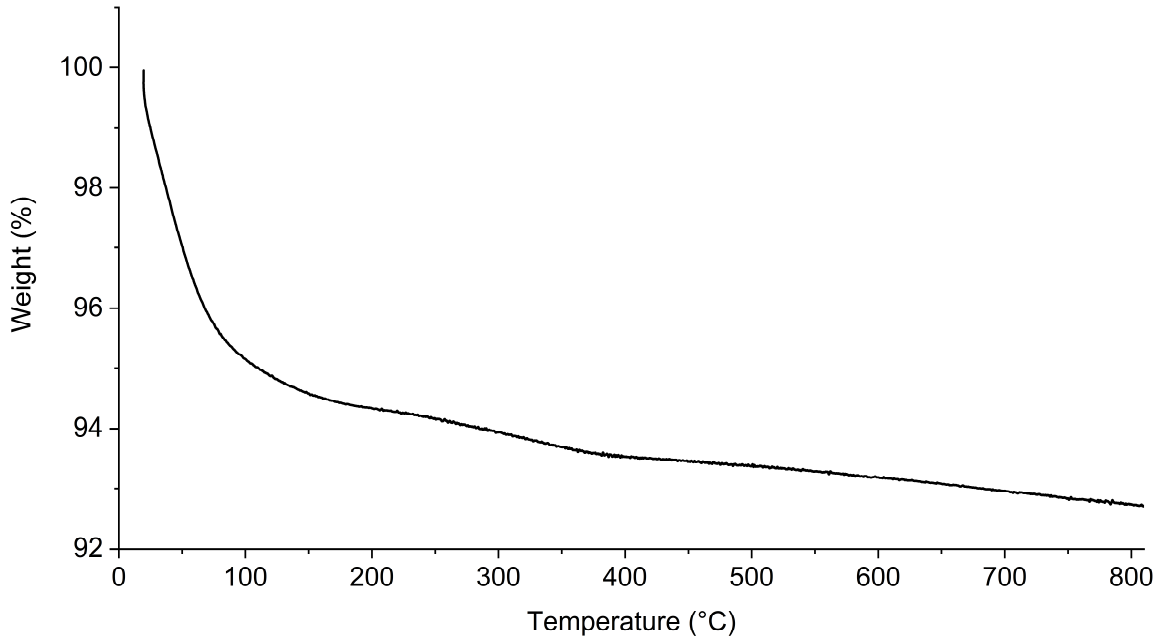

Figure S17c. Thermogravimetric analysis curve of ZSM-5-40.

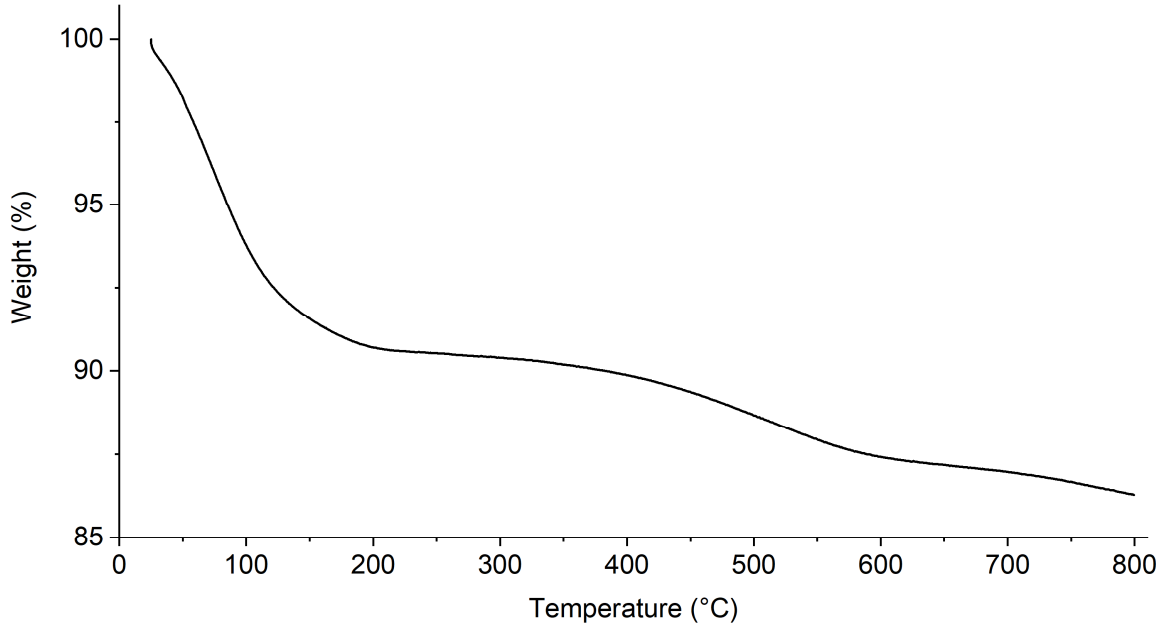

Figure S17d. Thermogravimetric analysis curve of MOR-10.

225

226

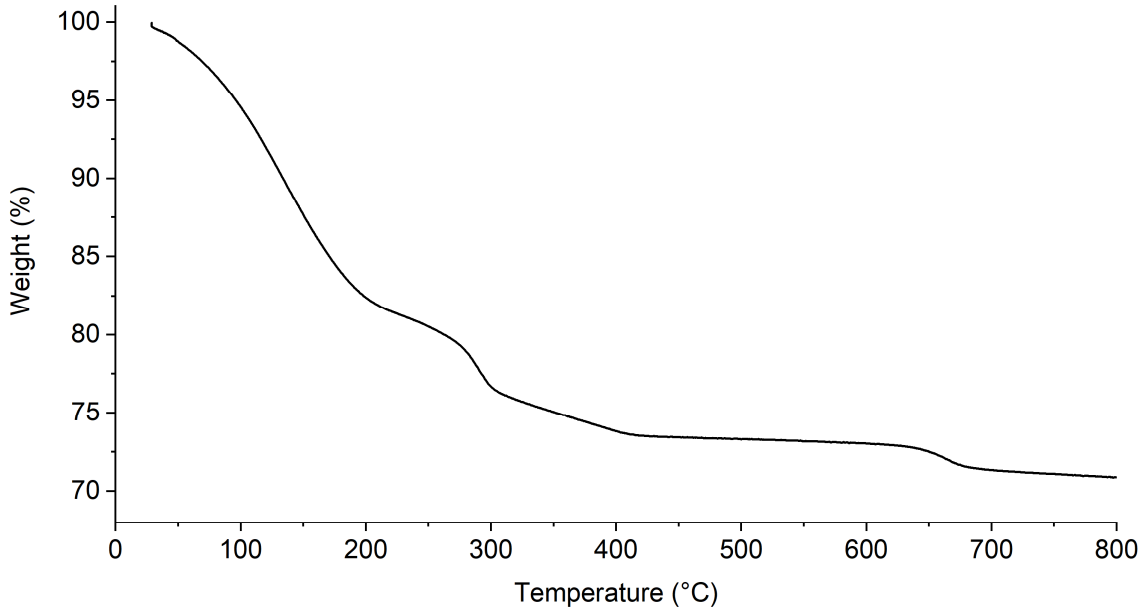

Figure S17f. Thermogravimetric analysis curve of FAU-Z.

227

228

NMR data

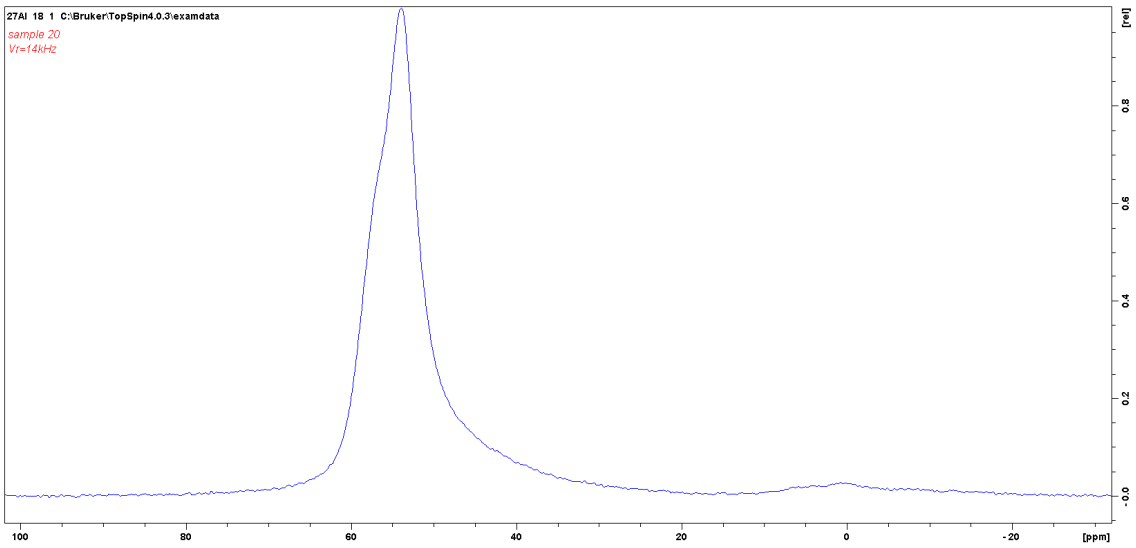

FigureS18a. ^{27}Al-NMR spectrum of BEA-12.

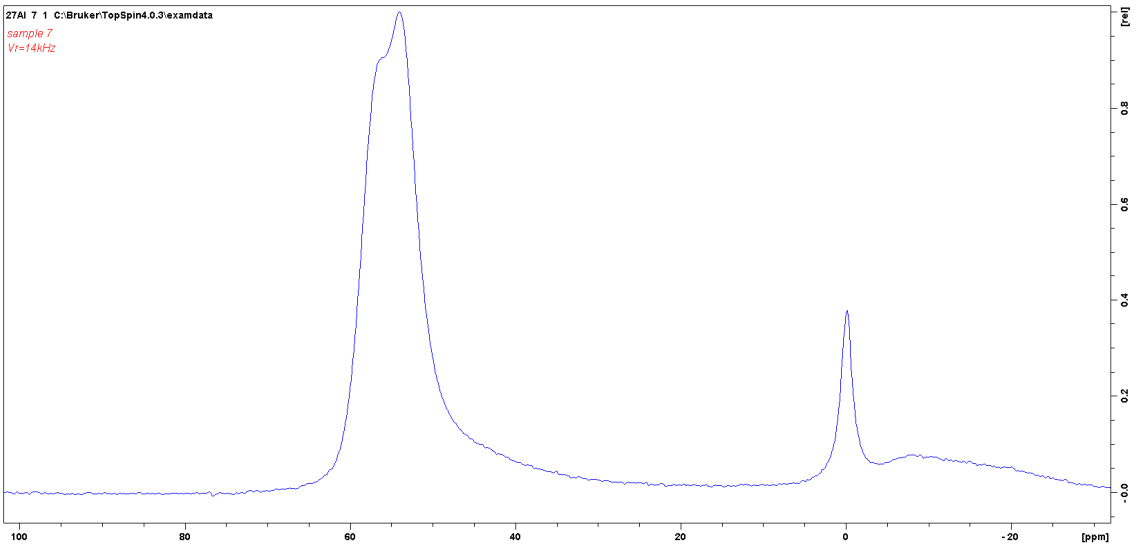

FigureS18b. ^{27}Al-NMR spectrum of BEA-19.

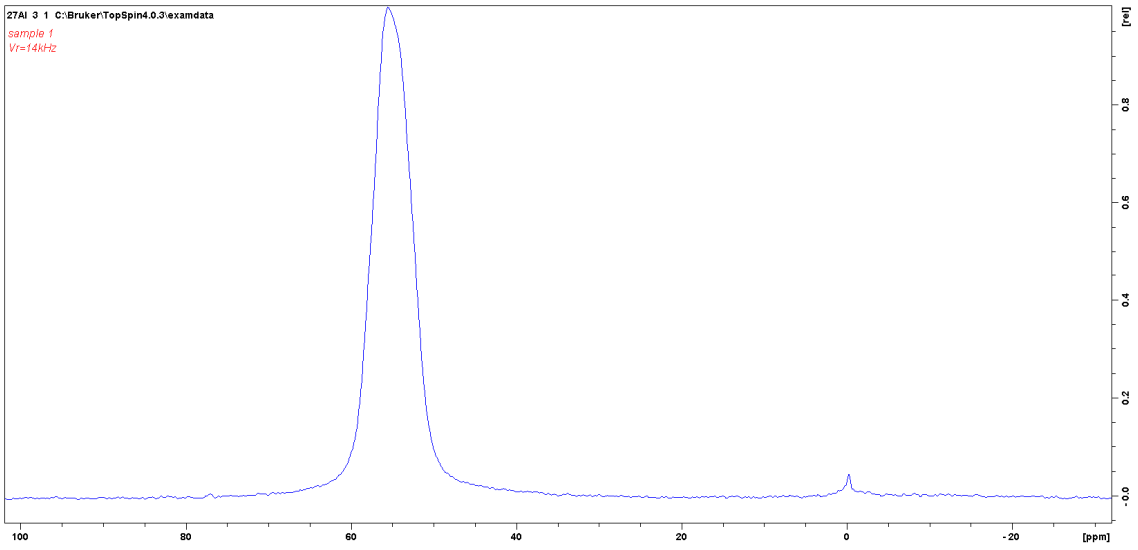

FigureS18c. ^{27}Al-NMR spectrum of ZSM-5-40.

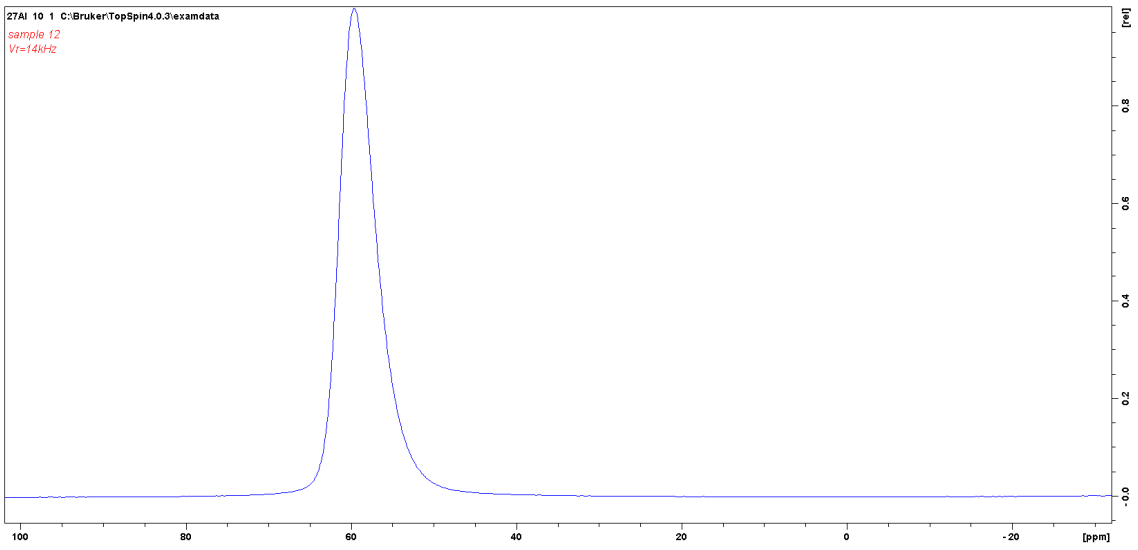

FigureS18d. ^{27}Al-NMR spectrum of MOR-10.

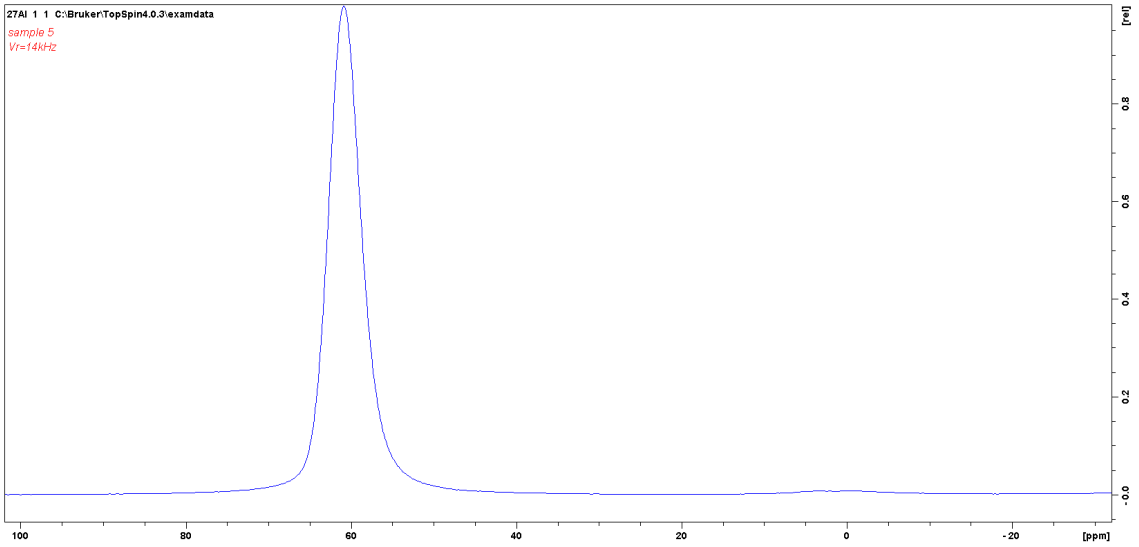

FigureS18e. ^{27}Al-NMR spectrum of Na-form of FAU-Z.

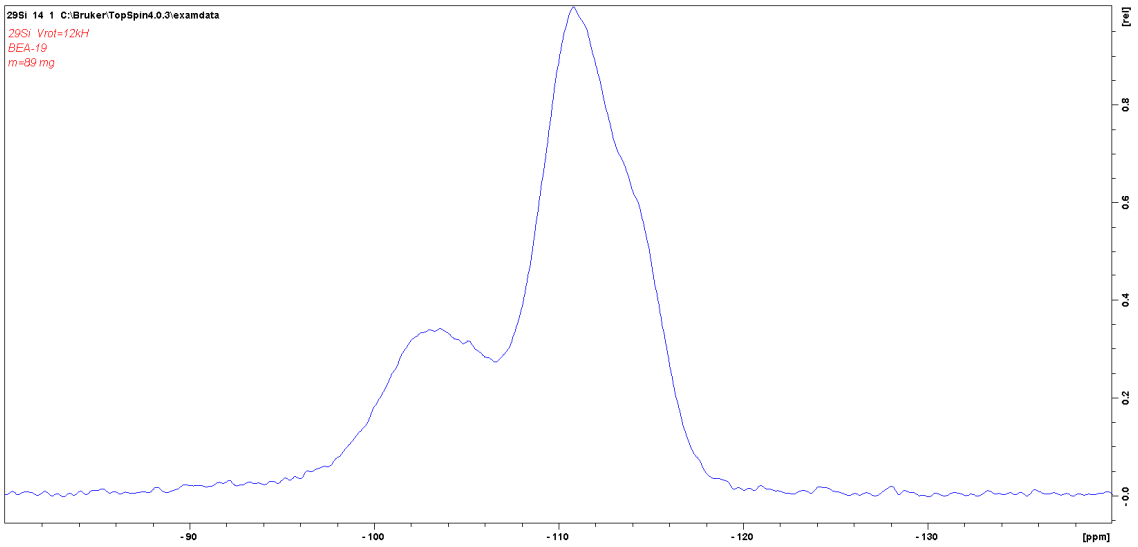

FigureS19a. ^{29}Si-NMR spectrum of BEA-19.

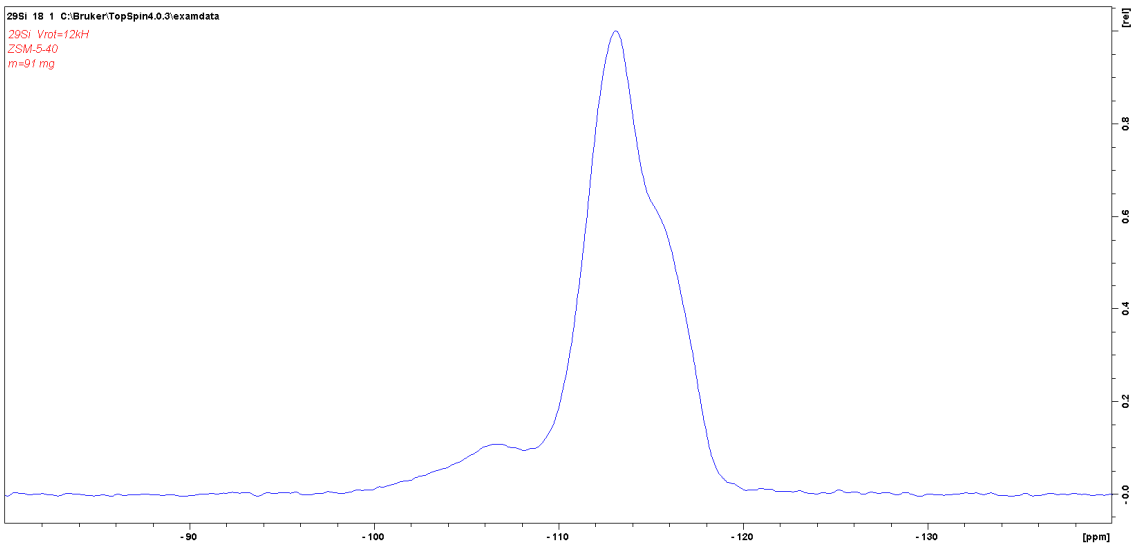

FigureS19b. ^{29}Si-NMR spectrum of ZSM-5-40.

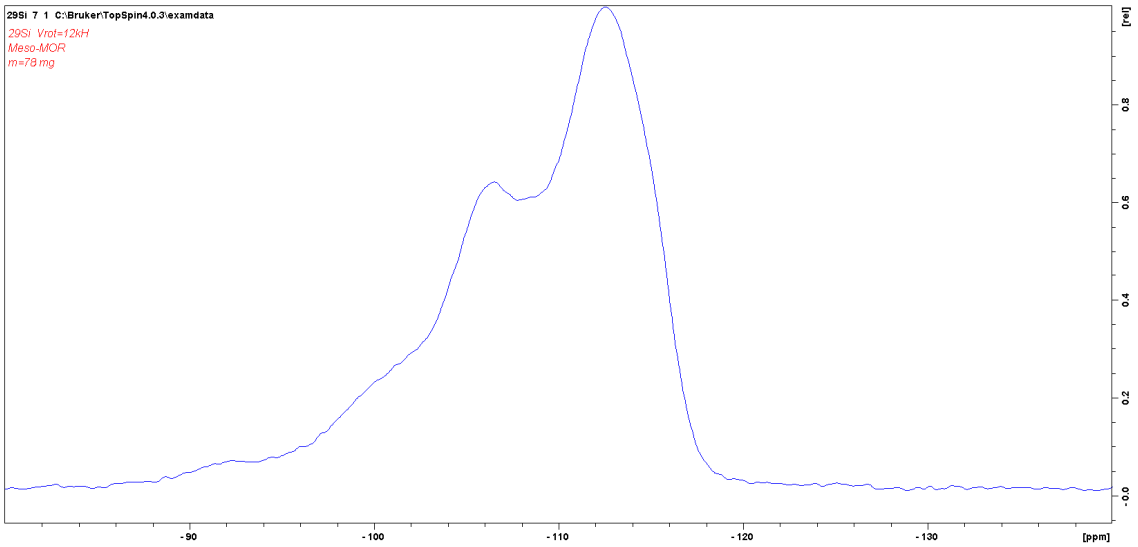

FigureS19c. ^{29}Si-NMR spectrum of MOR-10.

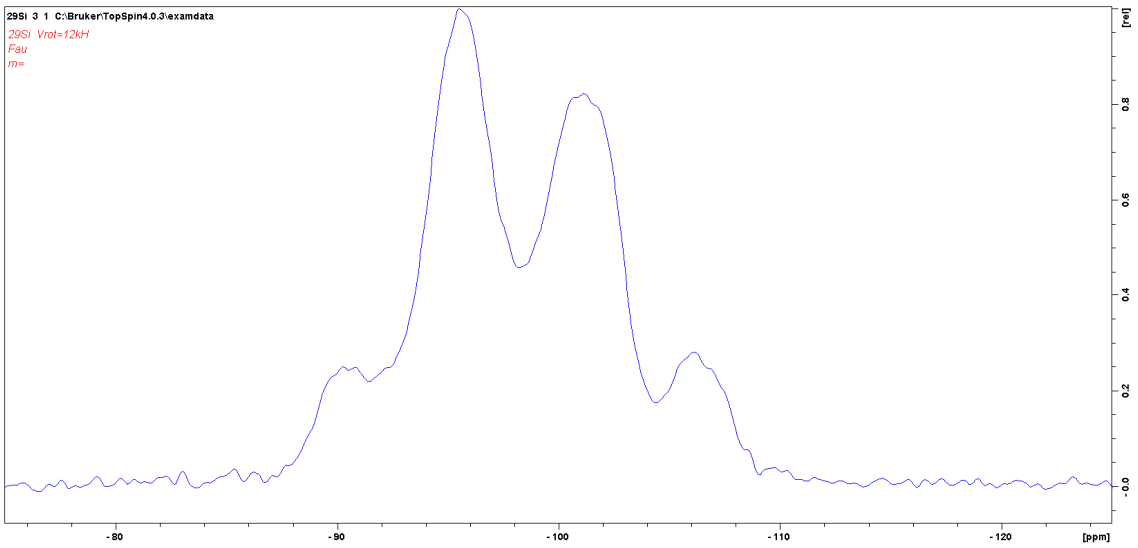

FigureS19d. ^{29}Si-NMR spectrum of Na-form of FAU-Z.

FTIR spectra of activated zeolites before and after Py adsorption. All spectra were collected at 200°C.

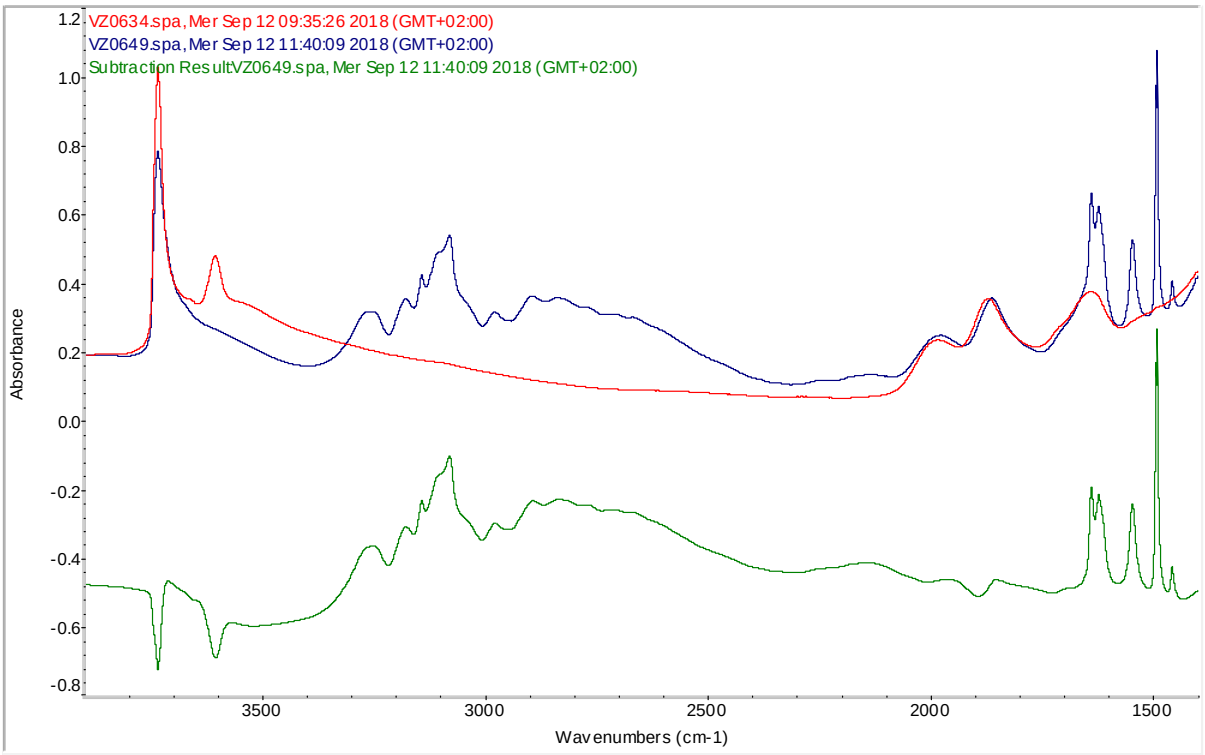

Figure S20a. FTIR spectra of BEA-19 before and after Py adsorption, and the difference spectrum.

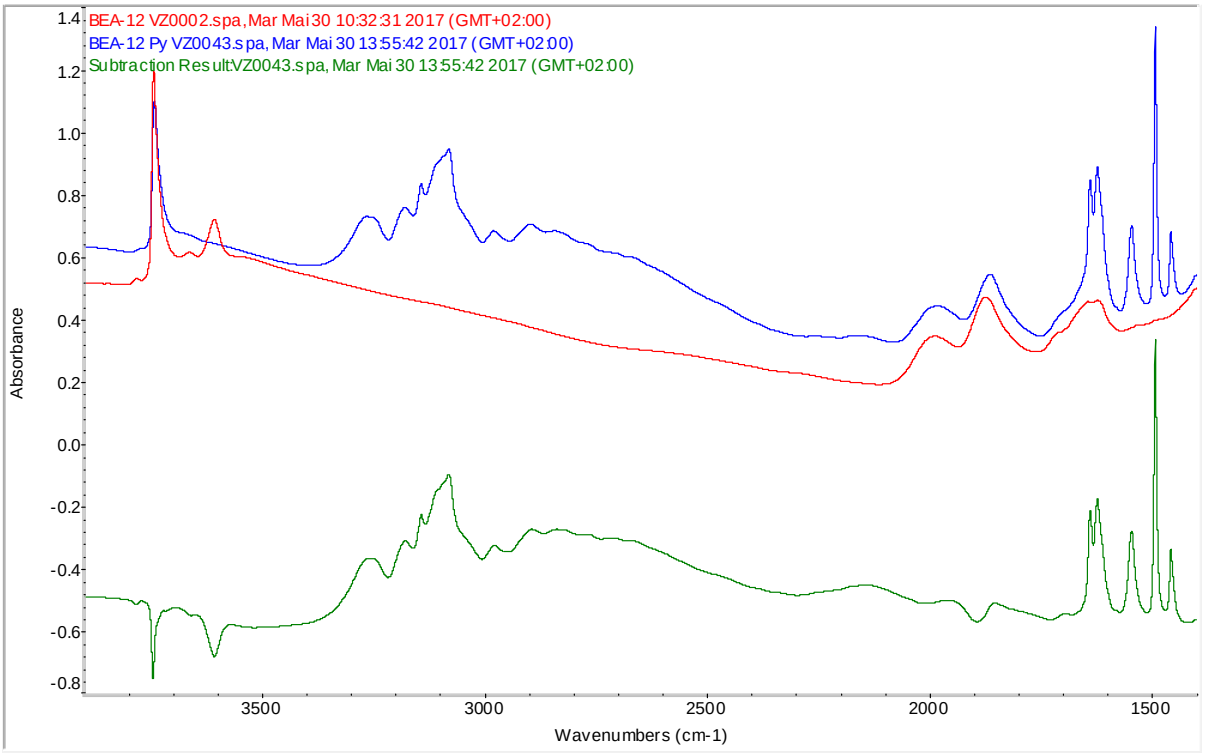

Figure S20b. FTIR spectra of BEA-12 before and after Py adsorption, and the difference spectrum.

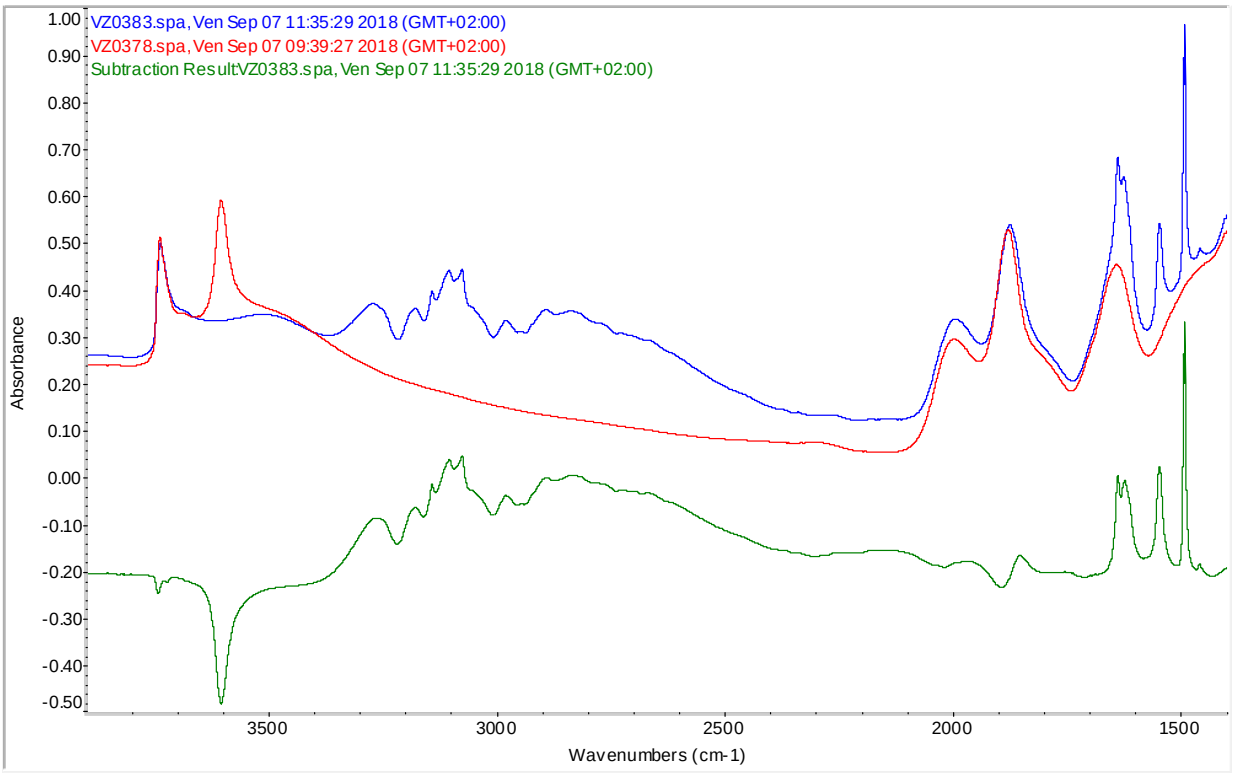

Figure S20c. FTIR spectra of ZSM-5-40 before and after Py adsorption, and the difference spectrum.

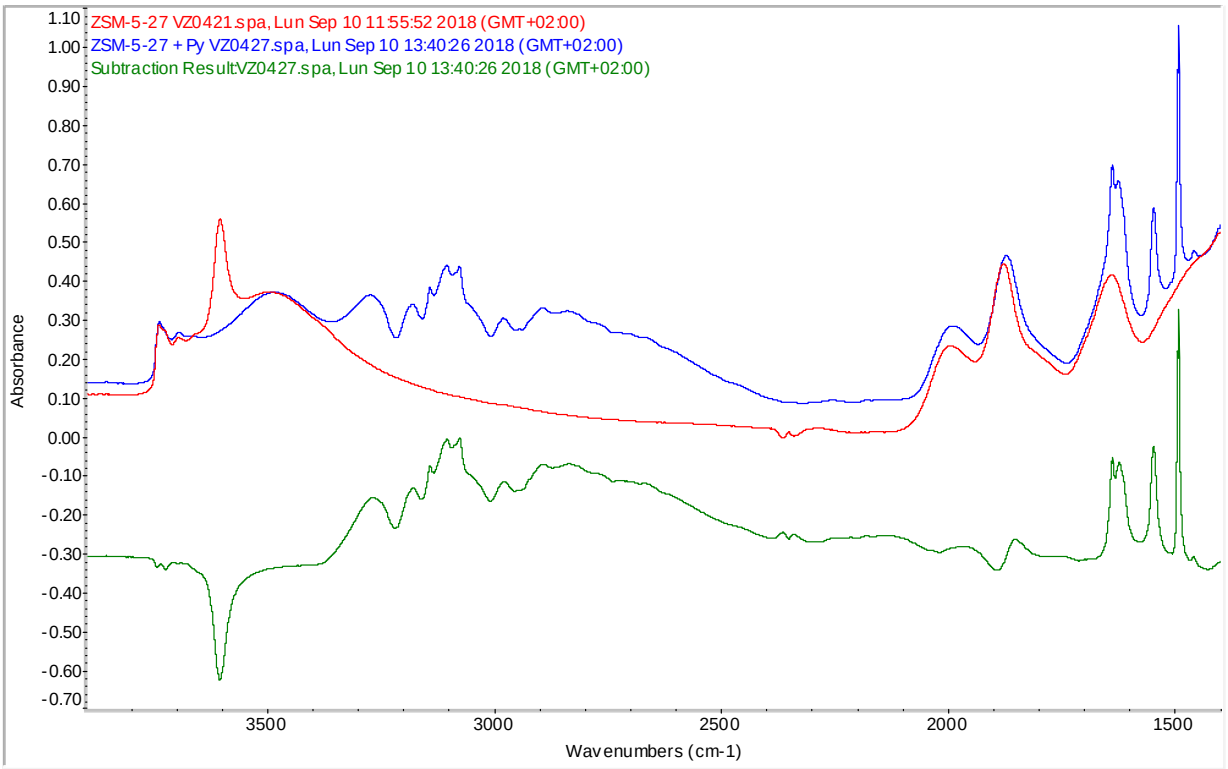

Figure S20d. FTIR spectra of ZSM-5-27 before and after Py adsorption, and the difference spectrum.

266

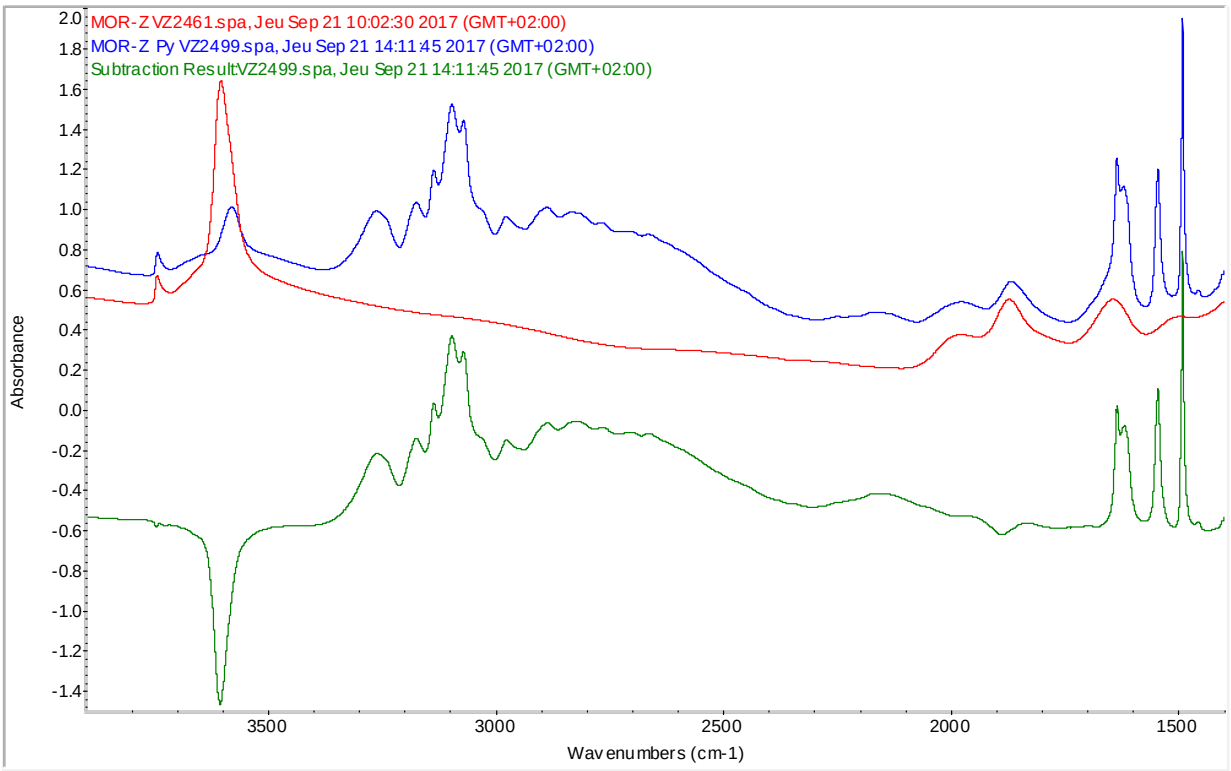

Figure S20e. FTIR spectra of MOR-10 before and after Py adsorption, and the difference spectrum.

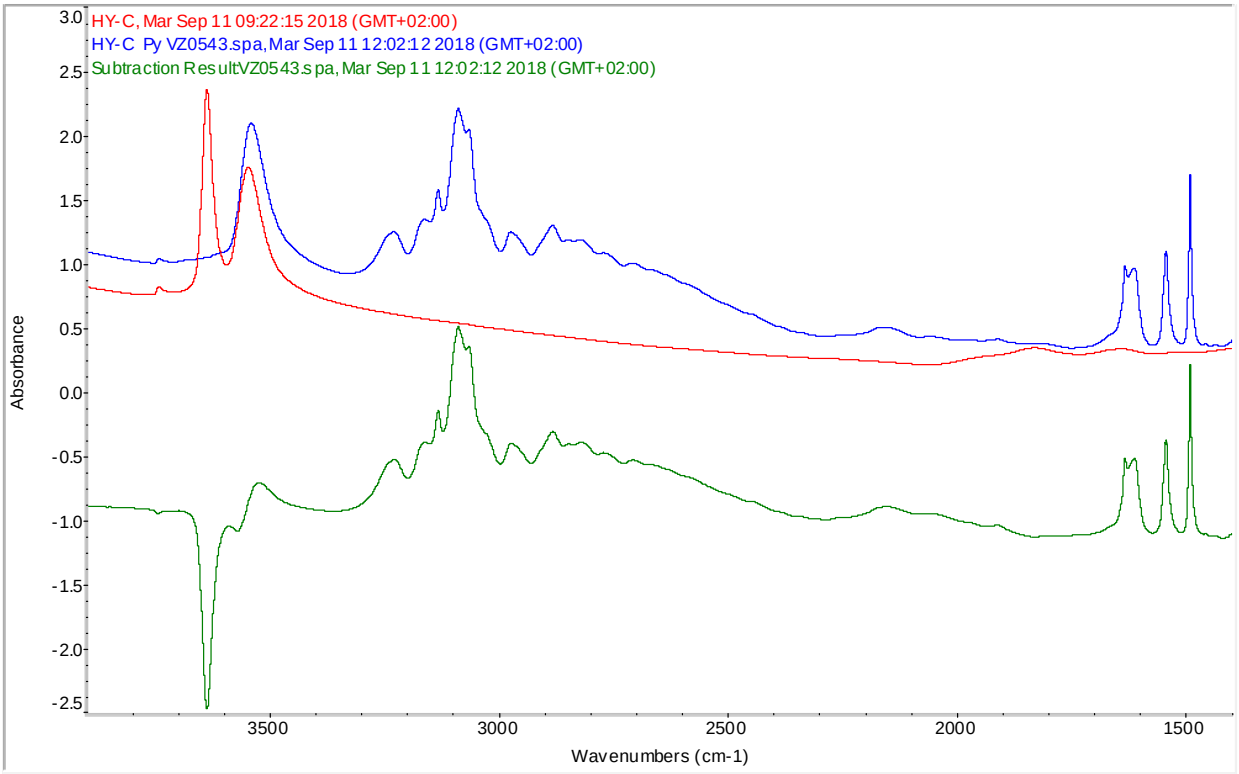

Figure S20f. FTIR spectra of FAU-C before and after Py adsorption, and the difference spectrum.

267

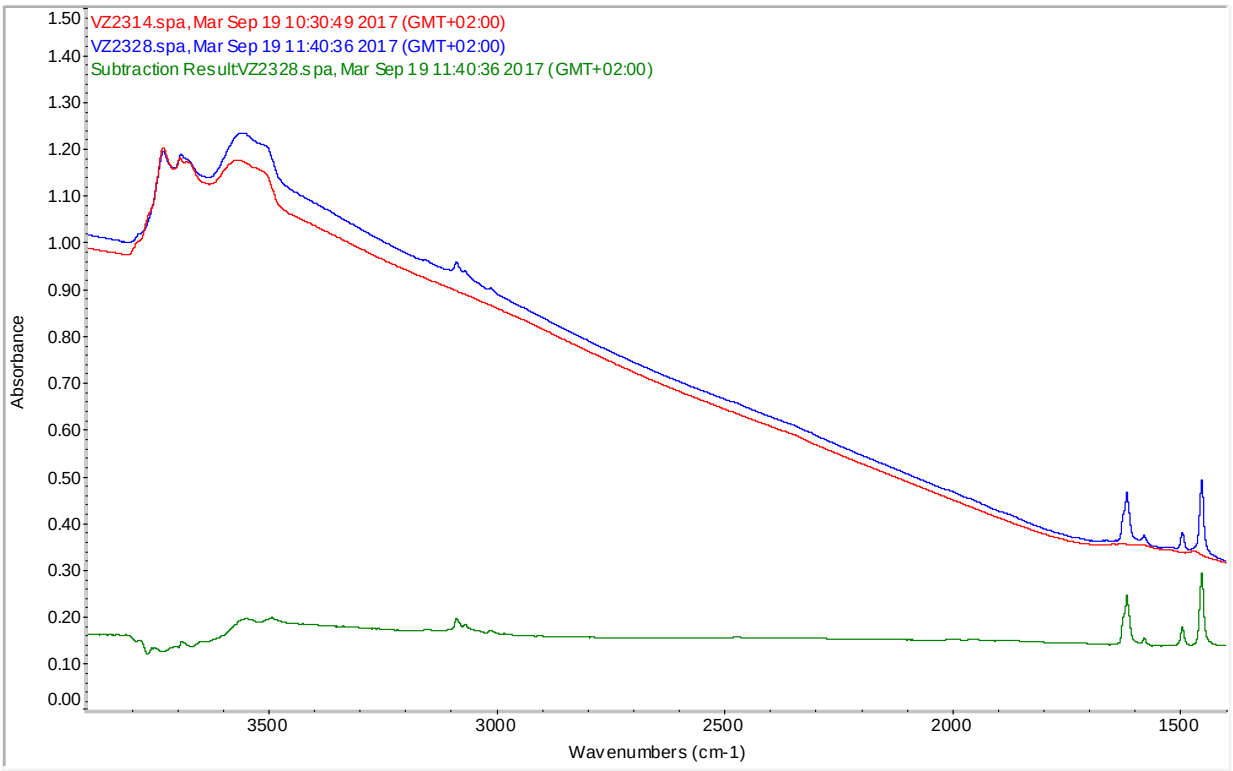

Figure S20g. FTIR spectra of ɔ-Al_2O_3 before and after Py adsorption, and the difference spectrum.

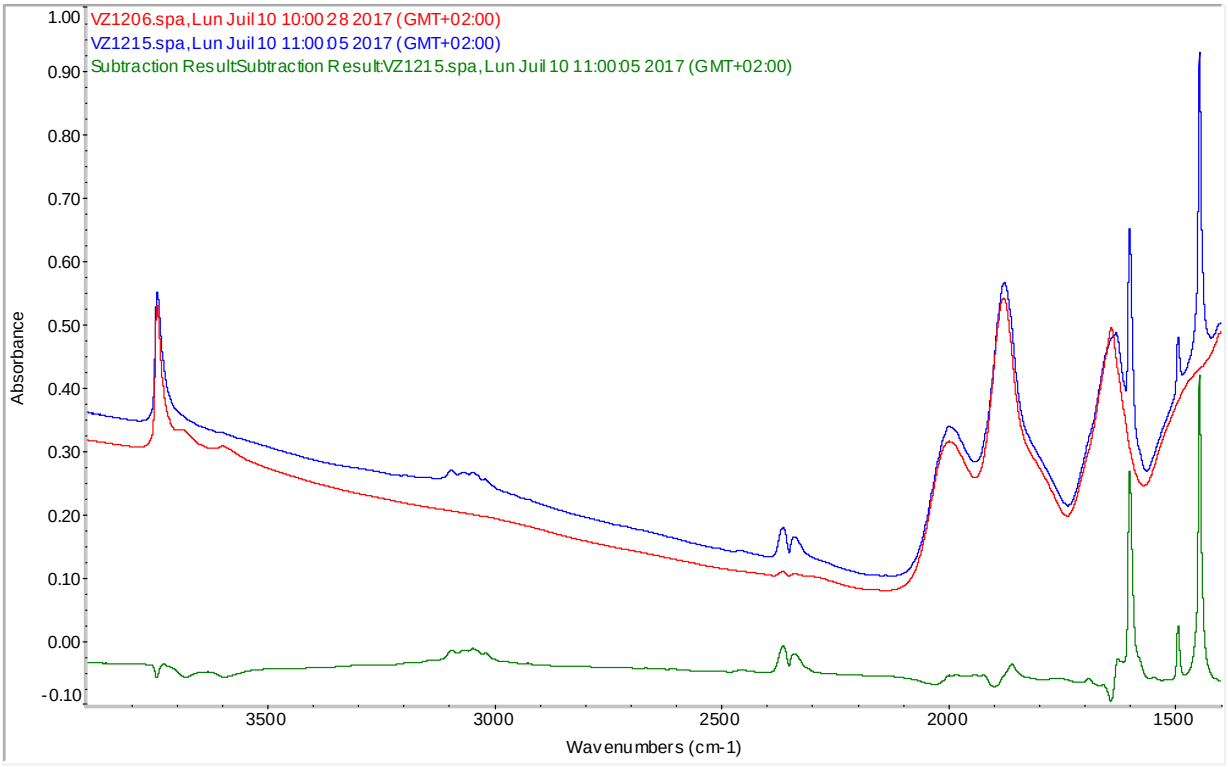

Figure S20h. FTIR spectra of NaZSM-5 before and after Py adsorption, and the difference spectrum.

268